

MINISTRY OF EDUCATION
AND TRAINING

VIETNAM ACADEMY OF SCIENCE
AND TECHNOLOGY

GRADUATE UNIVERSITY OF SCIENCE AND TECHNOLOGY



PHAM NGOC THU

**B-PHYSICS ANOMALIES
IN THE MINIMAL FLIPPED 3-3-1 MODEL**

Major: Theoretical and Mathematical Physics
Code: 9440103

SUMMARY OF DOCTORAL DISSERTATION IN PHYSICS

HA NOI - 2025

The work was completed at: Academy of Science and Technology, Vietnam Academy of Science and Technology

Scientific supervisors:

1. Supervisor: Assoc. Prof. Dr. Do Thi Huong - Institute of Physics
2. Supervisor: Prof. Dr. Hoang Ngoc Long - Institute of Physics

Reviewer 1:

Reviewer 2:

Reviewer 3:

The thesis was defended before the Academy-level Doctoral Thesis Evaluation Council meeting at the Academy of Science and Technology, Vietnam Academy of Science and Technology at hour, day month year

Thesis can be found at:

1. Library of the Academy of Science and Technology
2. National Library of Vietnam

INTRODUCTION

Urgency of the Thesis

The Standard Model (SM) is a unified theory describing strong and electroweak interactions based on the gauge symmetry group $SU(3)_C \otimes SU(2)_L \otimes U(1)_Y$. However, several phenomena such as neutrino masses and mixing, dark matter, matter-antimatter asymmetry, and CP violation in strong interactions have demonstrated that the SM is insufficient for a comprehensive description of nature. This motivates the study of beyond Standard Model (BSM) extensions.

One important property of the SM is lepton flavor universality (LFU), whereby the W^\pm and Z bosons interact equally with the three lepton generations e, μ, τ . However, recent experimental data suggest possible LFU violation (LFUV), manifested through anomalies in semileptonic B meson decays: i) $b \rightarrow c$ transitions with ratios $R(D), R(D^0)$ from BaBar and LHCb deviating from SM predictions, and ii) $b \rightarrow s\ell^+\ell^-$ transitions with ratios R_K, R_{K^0} smaller than SM values ($\simeq 1$). These anomalies can be explained by BSM models featuring tree-level flavor-changing neutral currents (FCNC), such as the 3-3-1 models. The minimal 3-3-1 flipped model (MF331), with fermion sector as in F331 and scalar multiplets reduced to two triplets, can generate tree-level LFUV and explain these anomalies.

With the expectation of elucidating the aforementioned anomalies of current interest, we choose to investigate the topic: "*B-physics anomalies in the minimal 3-3-1 flipped model*".

Research Objectives of the Thesis

Within the MF331 model framework, investigate lepton flavor universality violation in the anomalous decay channels $b \rightarrow s\ell^+\ell^-$, $b \rightarrow c\ell^-\bar{\nu}_\ell$, and the transitions $s \rightarrow u, d \rightarrow u$ through one-loop corrections. From the explanatory results obtained, focus on the parameter space regions in the MF331 model.

Main Research Contents of the Thesis

Overview of the SM and several BSM models. Present lepton flavor universality in the SM. Lepton flavor universality violation in some flavor physics anomalies. General introduction to the MF331 model. Examine lepton flavor universality violation in the anomalous semileptonic decay channels $b \rightarrow s\ell^+\ell^-$, $b \rightarrow c\ell^-\bar{\nu}_\ell$, and the transitions $s \rightarrow u, d \rightarrow u$.

Chapter 1. Overview of Lepton-Quark Universality, the Standard Model, and new physics anomalies

In this chapter, we first briefly introduce the universality of lepton-quark currents, present an overview of the SM structure, and discuss the advantages and limitations of the SM. The universality of leptons in the SM and physical anomalies that violate lepton universality, along with experimental data, are also introduced.

1.1. Lepton-quark universality

The universality of lepton and quark flavors (or generations) confirms that physics occurs identically across generations. The universality of leptons and quarks was known even before the Standard Model, in the theory of weak 4-fermion interactions (V-A theory).

1.1.1. Pion decay

A pion can decay into a muon or an electron. The ratio

$$\frac{\Gamma(\pi^- \rightarrow e^- + \bar{\nu}_e)}{\Gamma(\pi^- \rightarrow \mu^- + \bar{\nu}_\mu)} = \left(\frac{m_e}{m_\mu} \right)^2 \left(\frac{m_\pi^2 - m_\ell^2}{m_\pi^2 - m_\mu^2} \right)^2, \quad (1.1)$$

is in perfect agreement with the experimental result 1.23×10^{-14} . The above observation shows that the interaction is of the form $V - A$ which allows a good fit for meson decay.

1.1.2. Cabibbo current

Cabibbo proposed that the hadronic current consists of the sum of two currents:

$$J_\mu^{(h)} = \cos \theta_c J_\mu^{(0)} + \sin \theta_c J_\mu^{(1)}$$

The d and s quarks are not eigenstates of the weak interaction operator. Instead, the weak interaction eigenstates are given by: $d' = \cos \theta_c d + \sin \theta_c s$, $s' = -\sin \theta_c d + \cos \theta_c s$.

More generally, in the presence of three generations of quarks, the weak eigenstates are related to the flavor eigenstates through the CKM (Cabibbo-Kobayashi-Maskawa) matrix:

$$\begin{pmatrix} d' \\ s' \\ b' \end{pmatrix} = V_{CKM} \begin{pmatrix} d \\ s \\ b \end{pmatrix}.$$

The Cabibbo theory established the universality of the quark-lepton interaction.

1.2. The Standard Model of particle physics

The Standard Model with its two parts - the Glashow-Weinberg-Salam (GWS) electroweak theory and quantum chromodynamics (QCD) - is based on the corresponding gauge symmetry groups $SU(2)_L \otimes U(1)_Y$ and $SU(3)_C$. In the SM, particles are arranged as follows: corresponding to transformations under gauge transformation groups,

$$\begin{aligned}\psi_{aL} &= \begin{pmatrix} \nu_{aL} & e_{aL} \end{pmatrix}^T \sim (1, 2, -1), \quad e_{aR} \sim (1, 1, -2), \\ Q_{aL} &= \begin{pmatrix} u_{aL} & d_{aL} \end{pmatrix}^T \sim (3, 2, 1/3), \quad u_{aR} \sim (3, 1, 4/3), \quad d_{aR} \sim (3, 1, -2/3)\end{aligned}(1.2)$$

and $a = 1, 2, 3$ is the generation index.

The Standard Model (SM) predicts the existence of 12 gauge bosons that mediate the strong interaction, electromagnetic interaction, and weak interaction. The strong and electromagnetic interactions are long-range interactions, and their mediating particles are massless. Specifically, the strong interaction involves 8 massless gauge bosons called gluons, which mediate the interaction. The electromagnetic interaction is mediated by the photon, A_μ . The weak interaction, on the other hand, is a short-range interaction, requiring the mediating particles to have mass: the two charged gauge bosons W^\pm and the neutral boson Z . However, mass terms for these gauge vector bosons are forbidden by the $SU(2)_L \times U(1)_Y$ symmetry. To generate mass for the weak interaction mediators, scientists propose that spontaneous symmetry breaking is necessary. In the SM, a Higgs doublet ϕ is introduced into the model: $\phi = \begin{pmatrix} \varphi^+ \\ \varphi^0 \end{pmatrix} \sim (1, 2, 1)$ are positive and neutral complex scalar fields, respectively.

1.2.1. Scalar Mass Spectrum

After spontaneous symmetry breaking, the scalar potential yields a single physical field, H , with mass: $m_H = \sqrt{2\mu^2} = \sqrt{2\lambda}v$. The remaining scalar fields, ϕ^+ and ξ^i , are massless and are identified as the Goldstone bosons. These are absorbed by the gauge fields W^\pm and Z via the Higgs mechanism, providing the longitudinal components of the corresponding massive gauge bosons.

1.2.2. Gauge Boson Mass Spectrum

The two charged gauge bosons are defined as: $W_\mu^\pm = \frac{1}{\sqrt{2}}(A_{1\mu} \mp iA_{2\mu})$, and acquire masses given by: $m_{W^\pm}^2 = \frac{g^2}{4}v^2$. Among the neutral gauge bosons, the field A_μ remains massless and is identified as the photon. The massive neutral boson Z has a mass: $M_Z = \frac{1}{2}v\sqrt{g^2 + g'^2}$.

1.2.3. Fermion mass spectrum

. The Yukawa Lagrangian $\mathcal{L}_{\text{Yukawa}}^{\text{lepton}}$ for leptons in the unitary gauge is

$$\mathcal{L}_{\text{Yukawa}}^{\text{lepton}} = - \sum_{a,b=1,2,3} h_{ab}^\ell \bar{e}_{aL} \frac{(v + H)}{\sqrt{2}} e_{bR} + h.c$$

$$= - \sum_{a,b=1,2,3} \left(\bar{e}_{aL} \mathcal{M}_{ab}^\ell e_{bR} + \bar{e}_{aL} \frac{\mathcal{M}_{ab}^\ell}{v} e_{bR} H \right) + h.c \quad (1.3)$$

where $\mathcal{M}_{ab}^\ell = h_{ab}^\ell \frac{v}{\sqrt{2}}$ is the mass mixing matrix, $V_L^{l\dagger} \mathcal{M}^\ell V_R^l = M^\ell$.

Since there are no right-handed neutrinos ν_R in the SM, neutrinos have zero mass. The SM forbids decay channels that transition from one lepton generation to another.

The expression of the Yukawa Lagrangian that generates mass for quarks

$$\begin{aligned} \mathcal{L}_{\text{Yukawa}}^{\text{mass}} &= - \sum_{a,b} \left(\bar{u}_{aL} \mathcal{M}_{ab}^u u_{bR} + \bar{d}_{aL} \mathcal{M}_{ab}^d d_{bR} \right) \\ &\quad - \sum_{a,b} \left(\bar{u}_{aL} \frac{\mathcal{M}_{ab}^u}{v} u_{bR} H + \bar{d}_{aL} \frac{\mathcal{M}_{ab}^d}{v} d_{bR} H \right) + h.c, \end{aligned} \quad (1.4)$$

with $\mathcal{M}_{ab}^{u,d} = h_{ab}^{u,d} \frac{v}{\sqrt{2}}$ being the quark mass mixing matrix.

1.2.4. Weak Interaction Currents in the Standard Model

The fermion Lagrangian in the unitary gauge can be rewritten as:

$$\mathcal{L}_{\text{lepton}} = \bar{\psi}'_L i\gamma^\mu \partial_\mu \psi'_L + \bar{e}'_R i\gamma^\mu \partial_\mu e'_R + g \vec{J}_\mu \vec{A}'^\mu + \frac{g'}{2} J_\mu^Y B'^\mu, \quad (1.5)$$

Charged current interaction:

$$\mathcal{L}_{CC}^{\text{lepton}} = g (J_\mu^1 A'^{1\mu} + J_\mu^2 A'^{2\mu}) = \frac{g}{\sqrt{2}} (J_\mu^- W^{-\mu} + J_\mu^+ W^{-\mu}) \quad (1.6)$$

with $J_\mu^\pm = J_\mu^1 \pm i J_\mu^2$.

Neutral current interaction:

$$\mathcal{L}_{NC}^{\text{lepton}} = g' \cos \theta_W J_\mu^{\text{em}} A^\mu + \frac{g}{\cos \theta_W} (J_\mu^3 - \sin^2 \theta_W J_\mu^{\text{em}}) Z^\mu \quad (1.7)$$

Charged current interaction of quarks is

$$\mathcal{L}_{CC}^{\text{quark}} \frac{g}{2\sqrt{2}} \bar{u}'_i \gamma^\mu V_{ij} d'_j W_\mu^+ + h.c. \quad (1.8)$$

where the matrix $V = V_L^{u\dagger} V_L^d$ is a 3×3 unitary matrix, also called the CKM matrix. The charged current interaction of leptons preserves flavor number, but with quarks, it changes one quark generation to another quark generation.

The neutral current interaction of quarks has the form

$$\mathcal{L}_{NC}^{\text{quark}} = e J_\mu^{\text{em}} A^\mu + \frac{g}{\cos \theta_W} J_\mu^Z Z^\mu, \quad (1.9)$$

The neutral current interaction of fermions in the SM always preserves flavor.

1.3. Experiments on lepton universality in the Standard Model

1.3.1. The electroweak sector

Measurements of the branching ratios of $Z \rightarrow e^+ e^-$, $Z \rightarrow \mu^+ \mu^-$, $Z \rightarrow \tau^+ \tau^-$ are equal, completely consistent with the predictions of the SM.

LEP, Tevatron, and LHC experiments have also performed precise measurements using W boson decay. All experimental results are consistent with LU.

1.3.2. Decay of Quarkonia

The leptonic decay of quarkonium resonances can also be used to test lepton universality (LU). The most precise test is obtained from the branching ratio, $J/\psi \rightarrow e^+e^-$ and $J/\psi \rightarrow \mu^+\mu^-$: $\frac{\Gamma(J/\psi \rightarrow e^+e^-)}{\Gamma(J/\psi \rightarrow \mu^+\mu^-)} = 1.0016 \pm 0.0031$, which is in good agreement with LU.

1.4. Standard Model contributions to new physics anomalies, violation of lepton universality

1.4.1. Anomalies in the decay channel $b \rightarrow c\ell^-\bar{\nu}_\ell$

The ratios $R(D), R(D^{(*)})$ for quark transition V_{cb} are defined as the branching ratio between third-generation leptons and first and second generations:

$$R(D) = \frac{\mathcal{B}(B \rightarrow D\tau\nu_\tau)}{\mathcal{B}(B \rightarrow Dl\nu_l)}, \quad R(D^{(*)}) = \frac{\mathcal{B}(B \rightarrow D^{(*)}\tau^-\bar{\nu}_\tau)}{\mathcal{B}(B \rightarrow D^{(*)}l^-\bar{\nu}_l)} \quad (1.10)$$

Most recently, these ratios have been averaged in as

$$R(D^{(*)})^{\text{SM}} = 0.254 \pm 0.005, \quad R(D)^{\text{SM}} = 0.298 \pm 0.008, \quad (1.11)$$

The global average of experimental results, extracted from the most recent LHCb announcement on $R(D), R(D^{(*)})$, gives the value.

$$R(D^{(*)})^{\text{Exp}} = 0.284 \pm 0.013_{\text{total}}, \quad R(D)^{\text{Exp}} = 0.356 \pm 0.029_{\text{total}}. \quad (1.12)$$

The SM prediction is lower than the measurement.

1.4.2. Anomalies in the Decay Channel $b \rightarrow s\ell^+\ell^-$

In the Standard Model (SM), there are no flavor-changing neutral currents (FCNC) at tree level. Since there are no tree-level contributions in the SM, FCNC decays provide higher sensitivity to the possible existence of new physics (NP). In the SM, the ratios R_K and R_K^* are approximately equal to 1.

LHCb has announced the measured value of $R_K:R_K^{\text{LHCb}}$ ($[1.1, 6] \text{ GeV}^2$) = $0.846^{+0.042+0.013}_{-0.039-0.012}$, with a deviation of 3.1σ from the Standard Model (SM) prediction of $\simeq 1$, providing evidence for lepton flavor universality violation in this decay channel.

Another ratio observed by LHCb and Belle,

$$R_{K^*} \equiv \frac{\text{Br}(B \rightarrow K^*\mu^+\mu^-)}{\text{Br}(B \rightarrow K^*e^+e^-)},$$

is measured in two regions of the squared invariant mass of the outgoing lepton pair,

$$R_{K^*}^{\text{LHCb}} = \begin{cases} 0.66^{+0.11}_{-0.07} (\text{stat}) \pm 0.03 (\text{syst}) & \text{with } 0.045 < q^2 < 1.1 \text{ GeV}^2/c^4, \\ 0.69^{+0.11}_{-0.07} (\text{stat}) \pm 0.05 (\text{syst}) & \text{with } 1.1 < q^2 < 6.0 \text{ GeV}^2/c^4. \end{cases}$$

These ratios are determined to be lower than the SM expectation with corresponding deviations of 2.1σ and 2.5σ .

However, with the combination of Run 1 and Run 2 data at LHCb, the precision of the two ratios R_K and R_{K^*} has been improved. The reported values of R_K and R_{K^*} are:

$$\begin{cases} R_K = 0.994^{+0.090}_{-0.082}(\text{stat})^{+0.027}_{-0.029}(\text{syst}) & \text{with } 0.045 < q^2 < 1.1 \text{ GeV}^2/c^4, \\ R_K = 0.949^{+0.042}_{-0.041}(\text{stat})^{+0.023}_{-0.023}(\text{syst}) & \text{with } 1.1 < q^2 < 6.0 \text{ GeV}^2/c^4 \end{cases} \quad (1.13)$$

with a deviation of 0.2σ from the SM prediction $\simeq 1$, and

$$R_{K^*}^{LHCb} = \begin{cases} 0.927^{+0.093}_{-0.087}(\text{sat})^{+0.034}_{-0.033}(\text{syst}) & \text{with } 0.045 < q^2 < 1.1 \text{ GeV}^2/c^4, \\ 1.027^{+0.072}_{-0.068}(\text{sat})^{+0.027}_{-0.027}(\text{syst}) & \text{with } 1.1 < q^2 < 6.0 \text{ GeV}^2/c^4. \end{cases}$$

These ratios also exhibit a deviation of 0.2σ from the SM prediction.

Experimental results for the ratios R_K and R_{K^*} have been shown to be quite close to the Standard Model (SM) predictions. However, experimental measurements of the ratios R_D and R_{D^*} have remained largely unchanged compared to analyses based on pre-2022 data. This necessitates waiting for further experimental results to test lepton flavor universality (LFU) and searching for other signs of new physics (NP) at future accelerators.

Although current experiments are not yet sufficient to confirm the precise violation of LFU, there are still many other limitations of the SM, such as neutrino mass, dark matter and dark energy, Big Bang and inflation, charge quantization, and the large hierarchy between the electroweak and Planck scales. Among these challenges, new physics anomalies at accelerators and exotic physics hypotheses, such as the number of fermion generations, mass hierarchy between generations, and B physics, are being actively explored and remain a hot topic of research.

1.5. Conclusion of Chapter 1

This chapter has presented an overview of lepton and quark flavor universality in the Standard Model (SM), the role of the CKM matrix and the Higgs mechanism in particle mass generation. Although the SM describes well the three fundamental interactions and agrees with most experimental data, it still cannot explain neutrino masses, dark matter, and some recent anomalies in B meson decays. Processes such as $b \rightarrow c\ell\bar{\nu}_\ell$ and $b \rightarrow s\ell^+\ell^-$ may be signs of lepton flavor universality violation, suggesting the existence of new interactions.

In the next section of this dissertation, we will introduce several BSM frameworks, including extensions of the particle spectrum and enlargements of the electroweak symmetry group, which could incorporate new interactions capable of explaining the observed violations of lepton flavor universality in these flavor physics anomalies.

Chapter 2. Lepton Flavor Universality Violation in Some Extended Models

Lepton Flavor Universality (LFU) violation mechanisms typically involve intergenerational lepton mixing or novel interactions that violate the universality of weak interactions. LFU violation mechanisms generally entail mixing between lepton generations or the emergence of new interactions beyond the Standard Model (SM). To explain this phenomenon, new physics models such as leptoquarks or gauge symmetry extensions featuring Z' bosons have been proposed.

2.1. Model with Leptoquarks

The leptoquark model is one of the leading candidates for addressing the anomalies in R_K, R_{K^*} and R_D, R_{D^*} . In this framework, leptoquarks are bosons that transform as triplets under the $SU(3)_C$ gauge group and are introduced as extensions to the Standard Model (SM). Leptoquarks carry both lepton and baryon numbers and mediate interactions between quarks and leptons. These interactions induce FCCC at tree level, providing an explanation for R_D, R_{D^*} , and FCNC at the one-loop level, contributing to an explanation for R_K, R_{K^*} , through their connection with the CKM and PMNS matrices.

2.2. 3-3-1 Models

We classify 3-3-1 models based on particle arrangements, universal according to leptons (normal) or universal according to quarks (flipped).

2.2.1. Normal 3-3-1 Model

The 3-3-1 model has several theoretical advantages, such as explaining the number of fermion generations being exactly three, accounting for the small masses of neutrinos, addressing the strong CP problem, charge quantization, and the unusually large mass of the top quark. There are multiple versions of 3-3-1 models, depending on the value of the parameter β in the electric charge operator: $Q = T_3 + \beta T_8 + N$ where T_3 and T_8 are the diagonal generators of $SU(3)_L$, and N is the $U(1)_X$ charge. In the normal version, the three lepton generations are arranged identically, so the extra neutral gauge boson Z' couples universally to all leptons. As a result, this version does not induce lepton flavor universality violation (LFUV) and therefore cannot explain the observed anomalies in B-meson decays such as R_K and R_{D^*} . To generate LFUV, other versions of the model must be considered — for example, the flipped 3-3-1 model.

2.2.2. Flipped 3-3-1 Model

In the flipped 3-3-1 model, the arrangement of lepton generations is non-homogeneous: the first generation transforms differently from the other two generations and from all three quark generations. This configuration eliminates tree-level Flavor-Changing Neutral Currents (FCNCs) in the quark sector while permitting tree-level FCNCs in the lepton sector. This leads to natural flavor-mixing effects in the lepton sector, such as: Decay processes like $\mu \rightarrow 3e$, $\mu \rightarrow e\nu_\mu\bar{\nu}_e$, Nuclear $\mu - e$ conversion processes, and Non-standard neutrino interactions with matter. Consequently, the flipped 3-3-1 model emerges as a suitable candidate to explain anomalies in B meson decay channels, particularly those associated with Lepton Flavor Universality Violation (LFUV).

2.3. Minimal Flipped 3-3-1 Model

2.3.1. Gauge symmetry and particle spectrum

The F331 model possesses a complex Higgs spectrum comprising three triplets and one sextet, leading to high risk of unwanted lepton flavor-violating interactions in Higgs decay channels. To address this issue, the Minimally Flipped 3-3-1 (MF331) model has been proposed. The model features the gauge symmetry group $SU(3)_C \otimes SU(3)_L \otimes U(1)_X$ with the electric charge operator and weak hypercharge defined by: $Q = T_3 + \frac{1}{\sqrt{3}}T_8 + X$, $Y = \frac{1}{\sqrt{3}}T_8 + X$, where T_3, T_8 are the diagonal generators of $SU(3)_L$, and X is the generator of $U(1)_X$.

$$\begin{aligned} \psi_{1L} &= \begin{pmatrix} \xi^+ & \frac{1}{\sqrt{2}}\xi^0 & \frac{1}{\sqrt{2}}\nu_1 \\ \frac{1}{\sqrt{2}}\xi^0 & \xi^- & \frac{1}{\sqrt{2}}e_1 \\ \frac{1}{\sqrt{2}}\nu_1 & \frac{1}{\sqrt{2}}e_1 & E_1 \end{pmatrix}_L \sim \left(1, 6, -\frac{1}{3}\right), \quad \psi_{\alpha L} = \begin{pmatrix} \nu_\alpha \\ e_\alpha \\ E_\alpha \end{pmatrix}_L \sim \left(1, 3, -\frac{2}{3}\right), \\ Q_{aL} &= \begin{pmatrix} d_a \\ -u_a \\ U_a \end{pmatrix}_L \sim \left(3, 3^*, \frac{1}{3}\right), e_{aR} \sim (1, 1, -1), E_{aR} \sim (1, 1, -1), \\ u_{aR} &\sim (3, 1, 2/3), d_{aR} \sim (3, 1, -1/3), U_{aR} \sim (3, 1, 2/3). \end{aligned} \quad (2.1)$$

The MF331 model was introduced, where the fermion content is the same as in the F331 model, but the Higgs sector is reduced to only two scalar triplets: $\rho = \begin{pmatrix} \rho_1^+ \\ \rho_2^0 \\ \rho_3^0 \end{pmatrix} \sim (1, 3, 1/3)$, $\chi = \begin{pmatrix} \chi_1^+ \\ \chi_2^0 \\ \chi_3^0 \end{pmatrix} \sim (1, 3, 1/3)$. The MF331 model helps prevent dangerous lepton flavor violation in Standard Model-like Higgs decay channels. Simultaneously, it can generate LFU violation at the tree-level approximation, directly related to recent anomalies observed at the LHC.

2.3.2. Scalar Sector

The physical mass states:

$$m_H^2 \simeq \frac{(4\lambda_1\lambda_2 - \lambda_3^2)v^2}{2\lambda_2}, \quad m_{H1}^2 \simeq 2\lambda_2 w^2, \quad m^2 H' \simeq \frac{\lambda_4}{2}(v^2 + w^2), \quad (2.2)$$

and the Higgs triplets, ρ, χ , are represented through the physical states in the form of

$$\rho \simeq \begin{pmatrix} G_W^+ \\ \frac{1}{\sqrt{2}}(v + H + iG_Z) \\ \frac{1}{\sqrt{2}}w' + H' \end{pmatrix}, \quad \chi \simeq \begin{pmatrix} G_X^+ \\ \frac{1}{\sqrt{2}}v' + G_Y^0 \\ \frac{1}{\sqrt{2}}(w + H_1 + iG_{Z'}) \end{pmatrix}, \quad (2.3)$$

where $G_{W,X,Y,Z,Z'}$ are the Goldstone bosons.

2.3.3. Fermion mass spectrum

The d-quarks gain masses via the following non-renormalizable Yukawa terms:

$$[\mathcal{M}_d]_{ab} = \frac{h_{ab}^d}{2\Lambda}(wv - w'v'). \quad (2.4)$$

The SM u -quarks, $u = (u_1, u_2, u_3)$, and new U -quarks, $U = (U_1, U_2, U_3)$, are mixed via the following mass matrix

$$\mathcal{M}_{\text{up}} = \frac{1}{\sqrt{2}} \begin{pmatrix} h^u v + s^u v' & h^U v' + s^U v \\ -h^u w' - s^u w & -h^U w - s^U w' \end{pmatrix} = \begin{pmatrix} M_u & M_{uU} \\ M_{Uu} & M_U \end{pmatrix}. \quad (2.5)$$

In the basis, $e_a^\pm, E_a^\pm, \xi^\pm$, the charged lepton mass matrix has the form:

$$\mathcal{M}_l = \begin{pmatrix} M_{ee} & M_{eE} & M_{e\xi} \\ M_{Ee} & M_{EE} & M_{E\xi} \\ M_{\xi e} & M_{\xi E} & M_{\xi\xi} \end{pmatrix}, \quad (2.6)$$

The physical neutrino states are related to the flavor states as follows

$$\nu' = (\nu'_1 \quad \nu'_2 \quad \nu'_3)^T_{L,R} = V_{L,R}^\nu (\nu_1 \quad \nu_2 \quad \nu_3)^T_{L,R} \quad (2.7)$$

2.3.4. Gauge Bosons

The model generates 3 physical states:

$$A = s_W A_3 + \left(\frac{c_W t_W}{\sqrt{3}} A_8 + c_W \sqrt{1 - \frac{t_W^2}{3}} B \right), \quad (2.8)$$

$$Z = c_W A_3 - \left(\frac{s_W t_W}{\sqrt{3}} A_8 + s_W \sqrt{1 - \frac{t_W^2}{3}} B \right), \quad (2.9)$$

$$Z' = \sqrt{1 - \frac{t_W^2}{3}} A_8 - \frac{t_W}{\sqrt{3}} B, \quad (2.10)$$

and their corresponding masses $\left(0, \frac{g^2 v^2}{4c_W^2}, \frac{g^2 [c_{2W}^2 v^2 + 4c_W^4 w^2]}{4c_W^2 (3 - 3s_W^2)}\right)$ where $c_W = \cos \theta_W, s_W = \sin \theta_W$, θ_W is the Weinberg angle defined by $s_W = \frac{\sqrt{3} t_X}{\sqrt{3 + 4t_X^2}}$ with $t_X = \frac{g_X}{g}$.

There is a slight mixing between two neutral gauge bosons, Z, Z' , with a mixing angle defined as follows $t_{2\varphi} = -\frac{c_{2W}\sqrt{1+2c_{2W}v^2}}{2c_W^4 w^2}$. There are six non-hermitian gauge boson states,

$$W^\pm = \frac{A_1 \mp iA_2}{\sqrt{2}}, X^\pm = \frac{A_4 \mp iA_5}{\sqrt{2}}, Y^{0,(0*)} = \frac{A_6 \mp A_7}{\sqrt{2}} \quad (2.11)$$

with the mass expressions given by $m_W^2 \simeq \frac{g^2 v^2}{4}, m_X^2 \simeq \frac{g^2 \omega^2}{4}, m_Y^2 \simeq \frac{g^2 (v^2 + \omega^2)}{4}$. The presence of vacuum expectation values (VEVs), v' and w' , leads to the mixing of the charged gauge bosons W^\pm and X^\pm : $W'_\mu = \cos \theta W_\mu - \sin \theta X_\mu, X'_\mu = \sin \theta W_\mu + \cos \theta X_\mu$ where θ is a small mixing angle defined by $t_{2\theta} \equiv \tan 2\theta = \frac{-2(w'v + wv')}{v^2 + v'^2 + w^2 + w'^2}$.

2.3.5. Charged Current and Neutral Current

$$\mathcal{L}^{\text{C.C.}} = J_W^{-\mu} W_\mu^+ + J_X^{-\mu} X_\mu^+ + J_Y^{0\mu} Y_\mu^0 + \text{H.c.}, \quad (2.12)$$

$$J_W^{-\mu} = -\frac{g}{\sqrt{2}} \left\{ \bar{\nu}_{aL} \gamma^\mu e_{aL} + \bar{u}_{aL} \gamma^\mu d_{aL} + \sqrt{2} \left(\xi_L^+ \gamma^\mu \xi_L^0 + \xi_L^- \gamma^\mu \xi_L^- \right) \right\}, \quad (2.13)$$

$$J_X^{-\mu} = -\frac{g}{\sqrt{2}} \left\{ \bar{\nu}_{aL} \gamma^\mu E_{aL} + \sqrt{2} \left(\bar{\nu}_{1L} \gamma^\mu E_{1L} + \bar{\xi}_L^+ \gamma^\mu \nu_{1L} \right) + \bar{\xi}_L^- \gamma^\mu e_{1L} - \bar{U}_{aL} \gamma^\mu d_{aL} \right\}, \quad (2.14)$$

$$J_Y^{0\mu} = -\frac{g}{\sqrt{2}} \left\{ \bar{e}_{aL} \gamma^\mu E_{aL} + \sqrt{2} \left(\bar{e}_{1L} \gamma^\mu E_{1L} + \bar{\xi}_L^- \gamma^\mu e_{1L} \right) + \bar{\xi}_L^0 \gamma^\mu \nu_{1L} + \bar{U}_{aL} \gamma^\mu u_{aL} \right\}. \quad (2.15)$$

$$\mathcal{L}^{\text{N.C.}} = -\frac{g}{2c_W} \bar{f} \gamma^\mu \left\{ g_V^Z(f) - g_A^Z(f) \gamma_5 \right\} f Z_\mu - \frac{g}{2c_W} \bar{f} \gamma^\mu \left\{ g_V^{Z'}(f) - g_A^{Z'}(f) \gamma_5 \right\} f Z'_\mu, \quad (2.16)$$

The neutral bosons Z and especially Z' interact differently with each fermion generation, leading to LFU violation. Although all three quark generations transform identically under the $SU(3)_L \times U(1)_X$ group, FCNCs can still emerge at the one-loop level – particularly in relation to the $b \rightarrow s$ transition.

| f | $g_V^{Z'}(f)$ | $g_A^{Z'}(f)$ | $g_L^{Z'}(f)$ | $g_R^{Z'}(f)$ |
|------------|---------------------------------------|------------------------------------|---------------------------------------|-------------------------------------|
| e_1 | $\frac{1-2c_{2W}}{2\sqrt{1+2c_{2W}}}$ | $-\frac{1}{2\sqrt{1+2c_{2W}}}$ | $\frac{-c_{2W}}{2\sqrt{1+2c_{2W}}}$ | $\frac{s_W^2}{\sqrt{1+2c_{2W}}}$ |
| e_α | $\frac{2-c_{2W}}{2\sqrt{1+2c_{2W}}}$ | $\frac{c_{2W}}{2\sqrt{1+2c_{2W}}}$ | $\frac{1}{2\sqrt{1+2c_{2W}}}$ | $\frac{s_W^2}{\sqrt{1+2c_{2W}}}$ |
| d_a | $-\frac{\sqrt{1+2c_{2W}}}{6}$ | $-\frac{1}{2\sqrt{1+2c_{2W}}}$ | $-\frac{2+c_{2W}}{6\sqrt{1+2c_{2W}}}$ | $\frac{s_W^2}{3\sqrt{1+2c_{2W}}}$ |
| U_a | $\frac{7c_{2W}-1}{6\sqrt{1+2c_{2W}}}$ | $\frac{c_W^2}{\sqrt{1+2c_{2W}}}$ | $\frac{1+5c_{2W}}{6\sqrt{1+2c_{2W}}}$ | $-\frac{2s_W^2}{3\sqrt{1+2c_{2W}}}$ |
| f | $g_V^Z(f)$ | $g_A^Z(f)$ | $g_L^Z(f)$ | $g_R^Z(f)$ |
| e_a | $-\frac{1}{2} + 2s_W^2$ | $-\frac{1}{2}$ | $-\frac{1}{2} + s_W^2$ | s_W^2 |
| d_a | $-\frac{1}{2} + \frac{2}{3}s_W^2$ | $-\frac{1}{2}$ | $-\frac{1}{2} + \frac{1}{3}s_W^2$ | $\frac{1}{3}s_W^2$ |
| U_a | $-\frac{4}{3}s_W^2$ | 0 | $-\frac{2}{3}s_W^2$ | $-\frac{2}{3}s_W^2$ |

Bảng 2.1: Some interaction vertices of Z and Z' with fermions.

2.4. Conclusion of Chapter 2

We emphasize that in the Standard Model (SM), the semileptonic decay process $b \rightarrow c\ell^+\bar{\nu}_\ell$ is mediated by the charged current at tree level, whereas the decay process $b \rightarrow s\ell^+\ell^-$ is associated with the neutral current and occurs only through one-loop corrections. Experimental results (2014) indicate a deviation of approximately 25% from the SM predictions for both processes. This suggests the possible existence of a light mediator particle. Several theoretical proposals have been put forward, including models based on extended gauge symmetries, leptoquarks, strong interactions, and effective field theory approaches, all of which can provide potential explanations. One such approach has been discussed earlier. Specifically, in non-universal gauge extensions of the SM, B-meson decay anomalies can be explained through non-trivial adjustments of the scalar and gauge field parameters as well as mixing effects, while gauge mixing effects are suppressed. The minimal flipped 331 (MF331) model offers a viable explanation for the observed deviations from SM expectations in B-meson decays. The MF331 model retains all the advantages of the 331 model, including solutions for dark matter, neutrino mass generation, cosmic inflation, baryon asymmetry, the existence

of exactly three SM fermion families, strong CP conservation, and charge quantization. The key distinction of the MF331 model from other versions of the 331 framework lies in the arrangement of fermions within each generation. In the F331 model, the first-generation leptons transform as a sextet under $SU(3)_L$, while the remaining two lepton generations and all three quark generations transform as triplets. Consequently, the model predicts non-universal interactions between SM leptons and new particles (new fermions and new gauge bosons), naturally providing solutions to explain the observed anomalies in B-meson decays.

Chapter 3. Lepton universality violation processes in the minimal flipped 3-3-1 model

3.1. Lepton universality violation in $b \rightarrow s\ell^+\ell^-$

The MF331 model permits LFU violation through neutral current and charged current interactions, with the capability to explain experimental anomalies in the decay ratios R_K , R_{K^*} , R_D , and R_{D^*} , which constitute one of the verification channels for the existence of new physics beyond the SM.

3.1.1. The effective Hamiltonian for decay processes induced by transitions $b - s$

In the MF331 model, the transition processes $b \rightarrow s\ell^+\ell^-$ are determined by dimension-six operators, $\mathcal{O}_{7,8,9,10}$. The corresponding effective Hamiltonian can be written as:

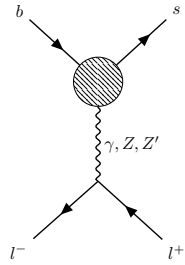
$$\mathcal{H}_{eff} = -\frac{4G_F}{\sqrt{2}} V_{tb} V_{ts}^* \times \sum_{i=7,8,9,10} \{C_i(\mu) O_i(\mu)\} + H.c., \quad (3.1)$$

The Wilson coefficients (WCs) are decomposed into the following contributions:

$$C_7 = C_7^{\text{eff-SM}} + \Delta C_7, \quad C_8 = C_8^{\text{SM}} + \Delta C_8, \quad C_9 = C_9^{\text{eff-SM}} + \Delta C_9, \quad C_{10} = C_{10}^{\text{SM}} + \Delta C_{10}. \quad (3.2)$$

The NP contribution to the aforementioned WCs can be decomposed as follows:

$$\begin{aligned} \Delta C_{9,10}^e &= \Delta C_{9,10}^{e,\gamma} + \Delta C_{9,10}^{e,Z} + \Delta C_{9,10}^{e,Z'} + \Delta C_{9,10}^{e,\text{box}}, \\ \Delta C_{9,10}^{\mu(\tau)} &= \Delta C_{9,10}^{\mu(\tau),\gamma} + \Delta C_{9,10}^{\mu(\tau),Z} + \Delta C_{9,10}^{\mu(\tau),Z'}, \\ \Delta C_{7,8} &= \Delta C_{7,8}^X. \end{aligned} \quad (3.3)$$



Hình 3.1: The penguin diagrams are induced by new charged gauge bosons W' , neutral bosons γ, Z, Z' , and the exotic boson X_μ^\pm . The dashed part represents the combination of the boson X^\pm and the new quark U inside the loop.

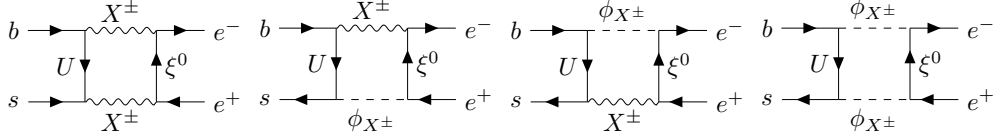
$$\begin{aligned}\Delta C_9^Z &= \frac{c_{2W} - 2s_W^2}{s_W^2} \left[\frac{-3x^2 c_W^2}{8(x-1)^2} \ln x + \frac{(x^2 + 5x - 3)c_{2W} + 3}{16(x-1)} \right], \\ \Delta C_{10}^Z &= -\frac{1}{s_W^2} \left[\frac{-3x^2 c_W^2}{8(x-1)^2} \ln x + \frac{(x^2 + 5x - 3)c_{2W} + 3}{16(x-1)} \right],\end{aligned}\quad (3.4)$$

Since the first-generation lepton transforms differently from the other two generations under the $SU(3)_L$ group, the gauge boson Z' interacts with it in a fundamentally different way compared to the other two generations. As a result, we obtain the following contributions for different generations:

$$\begin{aligned}\Delta C_9^{e,Z'} &= -\tilde{g}_V^{Z'}(e)f(x), \quad \Delta C_{10}^{e,Z'} = \tilde{g}_A^{Z'}(e)f(x), \\ \Delta C_9^{\mu(\tau),Z'} &= -\tilde{g}_V^{Z'}(\mu, \tau)f(x), \quad \Delta C_{10}^{\mu(\tau),Z'} = \tilde{g}_A^{Z'}(\mu, \tau)f(x),\end{aligned}\quad (3.5)$$

The different arrangements of fermion generations also lead to significantly different contributions to the Wilson coefficients (WCs). Only $C_{9,10}^e$ receive contributions from the box diagram shown in Figure (3.2). These additional contributions are given in the form:

$$\begin{aligned}\Delta C_9^{e,\text{box}} &= -\frac{1}{s_W^2} \frac{m_W^2}{m_X^2} \left\{ \frac{x^2[4 + (x-8)y]}{16(y-x)(x-1)^2} \ln x - \frac{xy[(y-4)^2 - 12]}{16(y-x)(y-1)^2} \ln y + \frac{x(-4+7y)}{16(y-1)(x-1)} \right\}, \\ \Delta C_{10}^{e,\text{box}} &= \frac{1}{s_W^2} \frac{m_W^2}{m_X^2} \left\{ \frac{x^2[4 + (x-8)y]}{16(y-x)(x-1)^2} \ln x - \frac{xy[(y-4)^2 - 12]}{16(y-x)(y-1)^2} \ln y + \frac{x(-4+7y)}{16(y-1)(x-1)} \right\}\end{aligned}\quad (3.6)$$



Hình 3.2: The box diagram contributes only to the first-generation lepton

The additional $bs\gamma$ interaction is generated by the photon penguin diagram induced by the new charged bosons X_μ^\pm , as shown in Figure 3.1. The electromagnetic currents of leptons couple to this interaction, leading to additional contributions to $C_{7,9}$.

$$\begin{aligned}\Delta C_9^\gamma &= \frac{4}{9} \ln x - \frac{x^2(5x^2 - 2x - 6)}{18(x-1)^4} \ln x - \frac{-19x^3 + 25x^2}{36(x-1)^3}, \\ \Delta C_7^X &= -\frac{8x^3 + 5x^2 - 7x}{24(x-1)^3} - \frac{x^2(2-3x)}{4(x-1)^4} \ln x.\end{aligned}\quad (3.7)$$

3.1.2. Lepton universality violation in $B^+ \rightarrow K^+ l^+ l^-$

The differential branching fraction for $B^+ \rightarrow K^+ l^+ l^-$:

$$\frac{d^2\Gamma(B^+ \rightarrow K^+ l^+ l^-)}{dq^2 d(\cos\theta)} = a(q^2) + b(q^2) \cos\theta + c(q^2) \cos^2\theta, \quad (3.8)$$

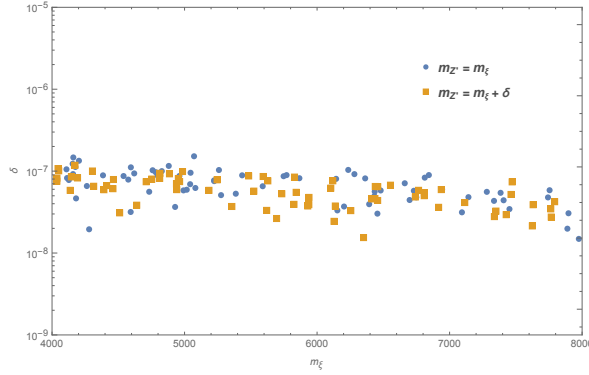
We obtain

$$a = \frac{\Gamma_0 \lambda^{3/2} \beta_l}{4} \left\{ |G|^2 + |\left(C_{10}^{\text{SM}} + \Delta C_{10}\right) f_+(q^2)|^2 + |(C_{10}^{\text{SM}} + \Delta C_{10}) f_0(q^2)|^2 \frac{4m_l^2}{\lambda q^2} (m_B^2 - m_K^2)^2 \right\},$$

$$\begin{aligned} b &= 0, \\ c &= -\frac{\Gamma_0 \lambda^{3/2} \beta_l^2}{4} \left\{ |G|^2 + \left| \left(C_{10}^{\text{SM}} + \Delta C_{10} \right) f_+(q^2) \right|^2 \right\} \end{aligned} \quad (3.9)$$

The LHCb experiment measured the ratio $R_K^{\text{LHCb}} ([1.1, 6] \text{ GeV}^2) = 0.846^{+0.042+0.013}_{-0.039-0.012}$ with a deviation of 3.1σ from the SM prediction, as described in the introduction. In the MF331 model, R_K also depends on unknown parameters, such as the masses of new particles m_{U_a} , m_{ξ^0} and $m_{Z'}$. The study examines two scenarios

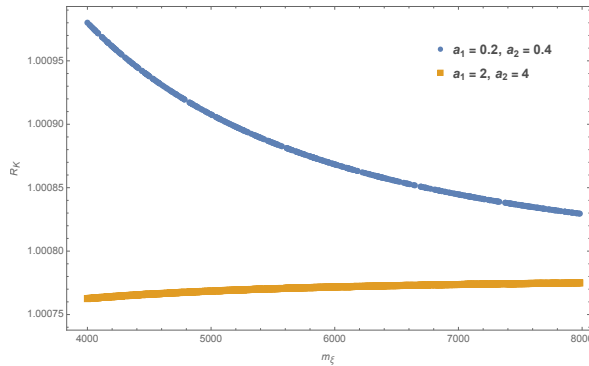
- Case 1: Mass Degeneracy $\Delta m \equiv m_{U,Z'} - m_{\xi^0} = \delta$, $\delta \ll 1$.
- Case 2: No Mass Degeneracy $m_U = a_1 m_{\xi^0}$, $m_{Z'} = a_2 m_{\xi^0}$, $a_{1,2} \sim \mathcal{O}(1)$.



Hình 3.3: The plot shows the viable parameter space obtained from the latest measurement, $R_K^{\text{LHCb}} ([1.1, 6] \text{ GeV}^2) = 0.846^{+0.042+0.013}_{-0.039-0.012}$. Here, $m_U = m_{\xi^0} + \delta$.

Results indicate:

- In scenario 1: R_K exhibits minimal dependence on the mass degeneracy between Z' and the new lepton m_{ξ^0} , but is significantly influenced by the mass degeneracy between new quarks and new leptons. The permissible range for δ spans from 10^{-6} to 10^{-7} , with the LHC constraint of $m_{Z'} > 4000$ GeV.
- In scenario 2: R_K asymptotically approaches 1, coinciding with the SM prediction and failing to explain the experimental value.

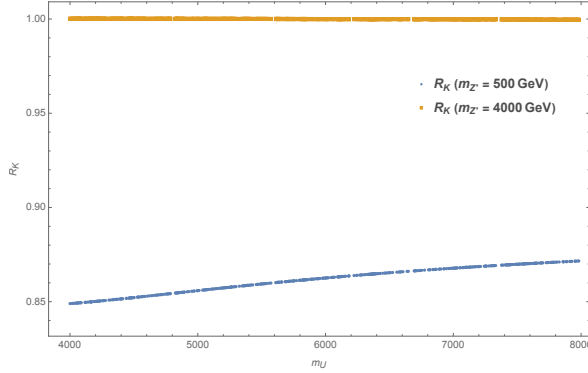


Hình 3.4: The ratio R_K as a function of the mass of new fermions in the case of no mass degeneracy.

The contributions from the penguin diagrams depend only on the parameter x , while the box diagram contributions depend on both y and x , particularly due to terms containing $\frac{1}{x-y}$. As a result, the box diagram contributions, $\Delta C_{9,10}^{\text{box-e}} \gg 1$, play a significant role in the R_K ratio. In the absence of mass degeneracy, the factor $\frac{1}{y-x} \simeq 1$, which leads to the cancellation of all diagrammatic contributions in Wilson coefficients by two factors $\frac{m_W^2}{m_X^2}$ and $\frac{m_W^2}{m_{Z'}^2}$. Thus, the R_K anomaly can only be explained in the case of mass degeneracy, with the box diagrams serving as the primary source of this anomaly.

We examine the contribution of penguin diagrams to the R_K anomaly induced by lepton flavor non-universal (LFU) interactions of the new gauge boson Z' with leptons, where $g^{Z'}(e) \neq g^{Z'}(\mu, \tau)$. Consequently, R_K is determined by the mass of the new boson Z' and the new quarks. Figure (3.5) illustrates the relationship between R_K and the new quark mass m_U , while fixing the mass of Z' .

If the new gauge boson has a mass of $m_{Z'} = 500$ GeV, then the ratio R_K can reach the experimental value. However, if $m_{Z'} = 4000$ GeV, the ratio will approach 1. On the other hand, LHC constraints indicate that the lower mass limit of Z' is several TeV, which means the value of R_K is close to the SM prediction $R_K^{\text{SM}} \simeq 1$. This implies that the contribution of box diagrams for the first lepton generation is a relevant source for explaining the R_K anomaly. Therefore, we conclude that the question of R_K in the MF331 model can only be addressed if both mass degeneracy of the new particles and the box diagram contributions for only the first-generation leptons are considered.



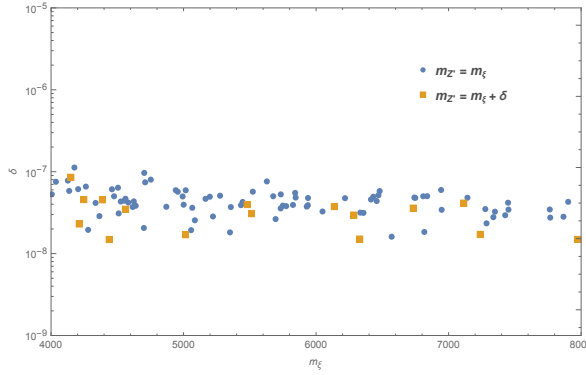
Hình 3.5:

3.1.3. Lepton Flavor Universality Violation in $B^0 \rightarrow K^{0*}l^+l^-$

The differential decay rate of the process $B^0 \rightarrow K^{0*}l^+l^-$ can be expressed as the sum of longitudinal and transverse polarization components

$$\frac{d\Gamma(B^0 \rightarrow K^{0*}l^+l^-)}{dq^2} = \frac{d\Gamma_L(B^0 \rightarrow K^{0*}l^+l^-)}{dq^2} + \frac{d\Gamma_T(B^0 \rightarrow K^{0*}l^+l^-)}{dq^2}. \quad (3.10)$$

The LHCb experiment has measured the ratio R_{K^*} in the invariant squared mass region $q^2 \in [1.1, 6]$ GeV 2 , obtaining the result $R_{K^*}^{\text{LHCb}} = 0.685^{+0.113}_{-0.069} \pm 0.047$, which deviates by approximately 2.5σ from the SM prediction. Now, we proceed to analyze the numerical results for the ratio R_{K^*} .



Hình 3.6:

Figure (3.6) illustrates the parameter space that satisfies experimental constraints by randomly sampling the parameters m_{ξ^0} and δ within the ranges $m_{\xi^0} \in [4000, 8000]$ GeV and $\delta \in [10^{-8}, 10^{-5}]$. The obtained parameter values, shown in Figure (3.6), overlap with the parameter space constrained by the measurement of R_K .

3.1.4. Conclusion

In the MF331 model, the interaction of the new neutral gauge boson Z' with the electron pair e^+e^- differs from its interaction with the $\mu^+\mu^-$ and $\tau^+\tau^-$ pairs, whereas the three generations of quarks couple to the Z' boson with the same strength. The photon and Z -penguin diagrams contribute equally to the Wilson coefficients (WCs) for all three lepton generations. However, the Z' -penguin diagrams provide different contributions between the first-generation leptons and the other two generations.

The new charged lepton current, $\bar{\xi}^0 \gamma^\mu e$, interacts with the new charged gauge boson X_μ^+ , leading to box diagrams that contribute only to the first-generation leptons in the Wilson coefficients. This explains why the MF331 model provides two possible sources of contributions to effective interactions that violate lepton flavor universality (LFU), allowing us to account for the anomalies in R_K and R_{K^*} . The contribution of the Z' -penguin diagram is negligible compared to the Standard Model (SM) contributions.

We demonstrate that the anomalies in R_K and R_{K^*} can be explained by the contributions from the box diagrams under the condition of mass degeneracy among the new particles.

3.2. Lepton Flavor Universality Violation in $b \rightarrow c$ Quark Transitions in the MF331 Model

3.2.1. Effects of New Physics on Charged Currents

The non-universal interactions of Z' and the charged bosons $X^\pm, Y^{0(0*)}$ with leptons are manifested through the charged current 2.3.5.

Lepton flavor universality (LFU) violation arises from charged currents associated with the complex gauge bosons X^\pm and Y^* . In addition to the differing couplings of lepton generations with these bosons, the interactions $\bar{\xi}^0 \gamma^\mu e_{1L} X_\mu^- + \bar{\xi}^0 \gamma^\mu \nu_{1L} Y_\mu^0$, which exist only for the

first generation, provide a plausible explanation for the observed deviations in LFU.

3.2.2. Effective Hamiltonian for Flavor-Violating $u^i - d^j$ Transitions

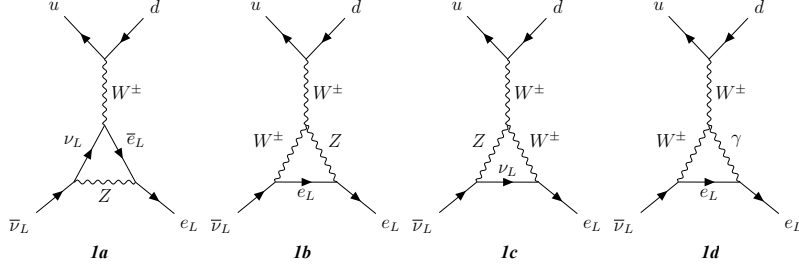
The contribution of the charged current to lepton-flavor-violating processes such as $u^i - d^j$ transitions is contained in the effective Hamiltonian:

$$\mathcal{H}_{eff} = \left[C_{\nu_a e_b}^{u_i d_j} \right] \left(\bar{u}'_{iL} \gamma^\mu d'_{jL} \bar{\nu}'_{aL} \gamma_\mu e'_{bL} \right). \quad (3.11)$$

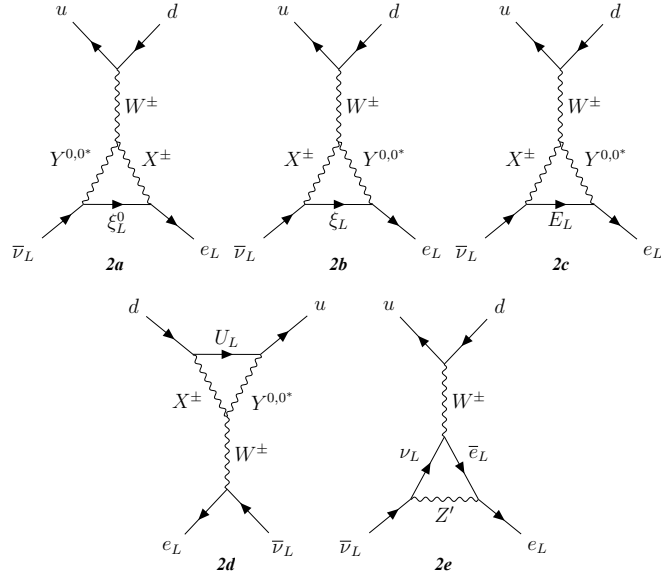
At tree level, the Wilson coefficients $\left[C_{\nu_a e_b}^{u_i d_j} \right]_{tree}$ decompose as follows:

$$\left[C_{\nu_a e_b}^{u_i d_j} \right]_{tree} = \left[C_{\nu_a e_c}^{u_i d_k} \right]_{SM} \left(\delta \left[C_{\nu_c e_b}^{u_k d_j} \right]_{W'_\mu} + \delta \left[C_{\nu_c e_b}^{u_k d_j} \right]_{X'_\mu} \right) \quad (3.12)$$

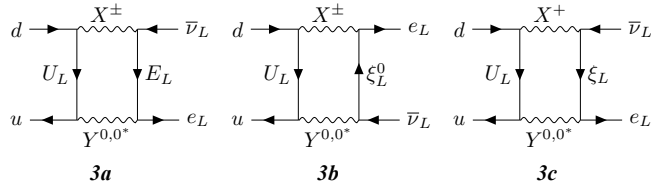
The non-universal interactions of both SM leptons and new leptons with the new gauge bosons also generate four-fermion interactions via penguin and box diagrams at the one-loop level, as illustrated in Figures (3.7), (3.8), and (3.9).



Hình 3.7: Penguin diagrams obtained from the SM



Hình 3.8: CPenguin diagrams obtained from new interactions



Hinh 3.9: Box diagrams

3.3. Lepton Flavor Universality Violation in $b \rightarrow c$ Transitions in the MF331 Model

3.3.1. Effects of New Physics on Charged Currents

The non-universal interactions of the Z' and the charged bosons $X^\pm, Y^{0(0*)}$ with leptons are manifested through the charged currents in Equation (2.3.5). Lepton flavor universality violation arises from the charged currents involving the exotic gauge bosons X^\pm, Y^* . In addition to the different couplings of the lepton generations with these exotic gauge bosons, the interactions $\bar{\xi}^0 \gamma^\mu e_{1L} X_\mu^- + \bar{\xi}^0 \gamma^\mu \nu_{1L} Y_\mu^0$ exist only for the first generation. This suggests a potential explanation for deviations in lepton universality (LU).

3.3.2. Effective Hamiltonian for Lepton-Flavor Violating $u^i - d^j$ Transitions

The contribution of the charged currents to lepton-flavor violating processes such as $u^i - d^j$ transitions is included in the effective Hamiltonian:

$$\mathcal{H}_{eff} = [C_{\nu_a e_b}^{u_i d_j}] (\bar{u}'_{iL} \gamma^\mu d'_{jL} \bar{\nu}'_{aL} \gamma_\mu e'_{bL}). \quad (3.13)$$

At the tree level, the Wilson coefficients $[C_{\nu_a e_b}^{u_i d_j}]_{tree}$ are decomposed as follows:

$$[C_{\nu_a e_b}^{u_i d_j}]_{tree} = [C_{\nu_a e_c}^{u_i d_k}]_{SM} \left(\delta [C_{\nu_c e_b}^{u_k d_j}]_{W'_\mu} + \delta [C_{\nu_c e_b}^{u_k d_j}]_{X'_\mu} \right). \quad (3.14)$$

The non-universal interactions of SM leptons and new leptons with the new gauge bosons also induce four-fermion interactions through penguin and box diagrams at the one-loop level, as illustrated in Figures (3.7), (3.8), and (3.9).

One-Loop Contributions Taking into account one-loop contributions:

$$[C_{\nu_a e_b}^{u_i d_j}] = [C_{\nu_a e_b}^{u_i d_j}]_{tree} + [C_{\nu_a e_b}^{u_i d_j}]_{penguin} + [C_{\nu_a e_b}^{u_i d_j}]_{box}. \quad (3.15)$$

The penguin diagram contribution is divided into two components:

$$[C_{\nu_a e_b}^{u_i d_j}]_{penguin} = [C_{\nu_a e_b}^{u_i d_j}]_{penguin}^{SM} + [C_{\nu_a e_b}^{u_i d_j}]_{penguin}^{NP}. \quad (3.16)$$

Box diagrams, shown in Figure (3.9), contribute to the Wilson coefficients as follows:

$$[C_{\nu_a e_b}^{u_i d_j}]_{box} = -\frac{4G_F}{\sqrt{2}} \frac{51g^2}{64\pi^2} \frac{m_W^2}{m_X^2 - m_Y^2} \left\{ [C_{\nu_a e_b}^{u_i d_j}]_{box}^E + [C_{\nu_a e_b}^{u_i d_j}]_{box}^{\xi^0} + [C_{\nu_a e_b}^{u_i d_j}]_{box}^\xi \right\}. \quad (3.17)$$

3.3.3. Study of Lepton Flavor Universality Violation in $b \rightarrow c$ Transitions

$$R(D^{(*)}) \equiv \frac{\Gamma(B \rightarrow D^{(*)}\tau\bar{\nu})}{\Gamma(B \rightarrow D^{(*)}l\bar{\nu})} = \frac{\sum_k |C_{3j}^{cb}|^2}{\sum_k (|C_{1k}^{cb}|^2 + |C_{2k}^{cb}|^2)} \times \left[\frac{\sum_k (|C_{1k}^{cb}|^2 + |C_{2k}^{cb}|^2)}{\sum_k |C_{3k}^{cb}|^2} \right]_{SM} \times R(D^{(*)})_{SM}. \quad (3.18)$$

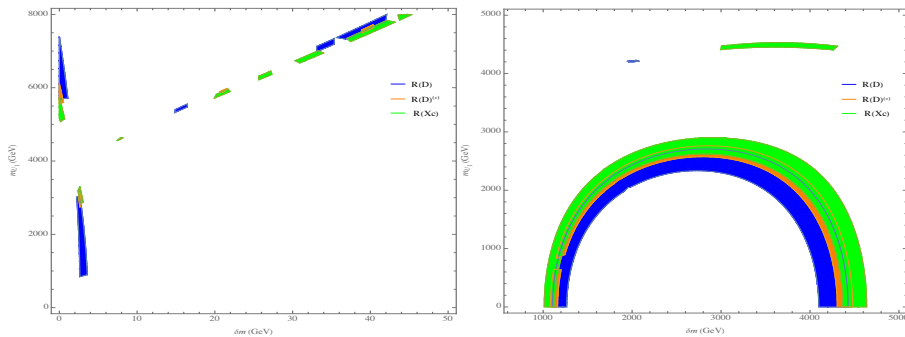
$$R(X_c) \equiv \frac{\Gamma(B \rightarrow X_c \tau\bar{\nu})}{\Gamma(B \rightarrow X_c l\bar{\nu})} = \frac{\sum_k |C_{3k}^{cb}|^2}{\sum_k |C_{1k}^{cb}|^2} \times \left[\frac{\sum_k |C_{1k}^{cb}|^2}{\sum_k |C_{3k}^{cb}|^2} \right]_{SM} \times R(X_c)_{SM}. \quad (3.19)$$

For numerical evaluation, we use the SM parameters and assume the new physics parameters as follows:

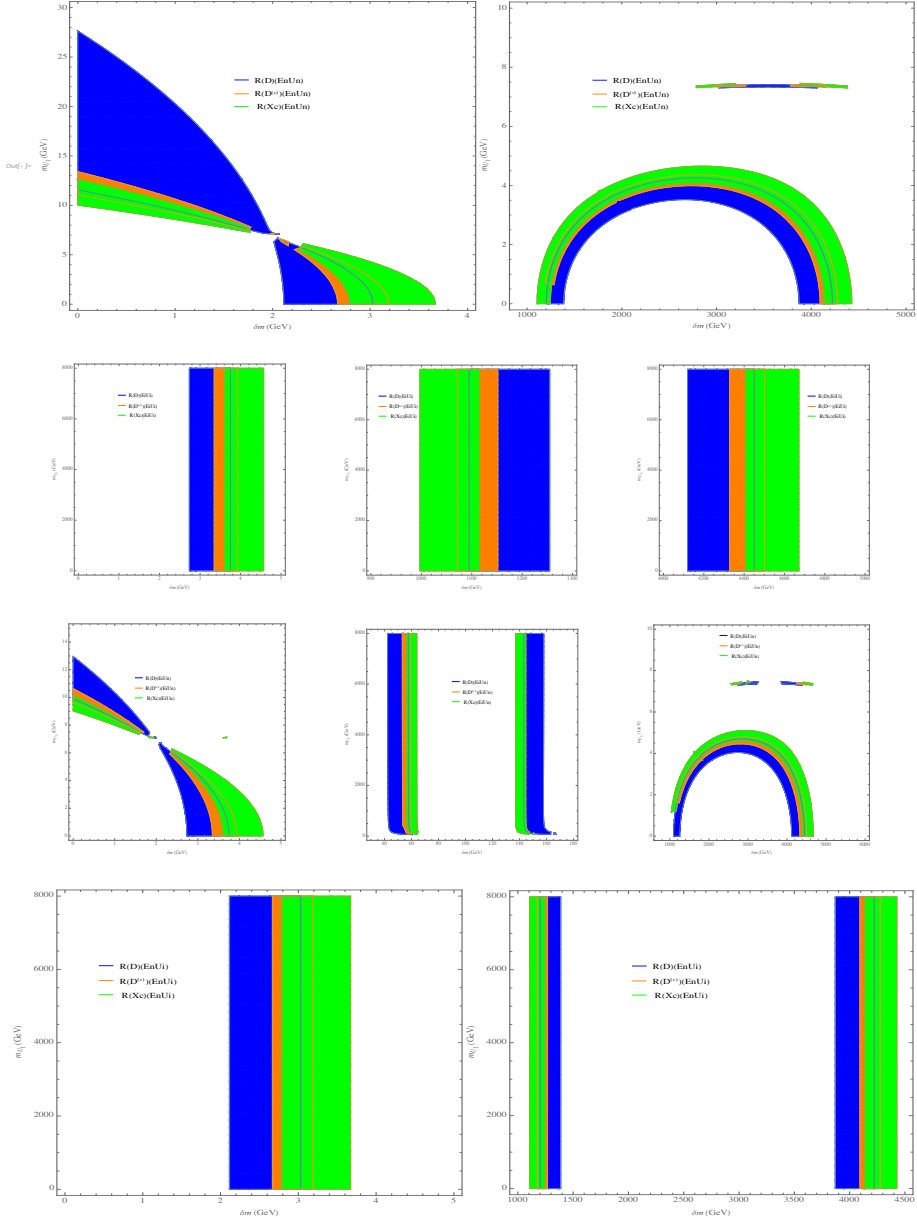
- The lepton and quark mixing matrices are given as follows: $V_L^l = V_L^u = V_L^U = V_L^E = \text{Diag}(1, 1, 1)$, $V_L^\nu = U_{\text{PMNS}}$, $V_L^d = V_{\text{CKM}}$. This corresponds to choosing a basis in which the mass matrices of the up-type quarks and charged leptons are diagonal, so that the observed quark and lepton mixing arises only from the down-type quarks and neutrinos, respectively.
- To satisfy the LHC constraints, the masses of the new gauge bosons are chosen as: $m_{Z'} = 4500$ GeV, $m_X = 4100$ GeV, $m_Y^2 = m_X^2 + m_W^2$.

Without loss of generality, we consider the mass hierarchy of the new fermions under four scenarios:

- Degenerate masses for new leptons and exotic quarks, with $m_{E_1} = m_{E_2} = m_{E_3}$ and $m_{U_1} = m_{U_2} = m_{U_3}$.
- Normal mass hierarchy ($E_n U_n$) where both new leptons and quarks follow SM-like generation scaling.
- Inverted mass hierarchy ($E_i U_i$) where both new leptons and quarks follow SM-like generation scaling.
- Mixed hierarchies with either normal lepton/inverted quark scaling ($E_n U_i$) or inverted lepton/normal quark scaling ($E_i U_n$).



Hình 3.10:



Hình 3.11:

In the first scenario, shown in the plots of Figure (3.10), we represent the parameter space in the $\delta m - m_{U_1}$ plane that satisfies the experimental constraints of $R(D)$, $R(D^*)$, and $R(X_c)$ using blue, orange, and green regions, respectively. We assume $m_{E_1} = m_{E_2} = m_{E_3}$ and $m_{U_1} = m_{U_2} = m_{U_3}$, with $m_\xi = m_{E_1} + \delta m$ and $m_{\xi^0} = m_{E_1} - \delta m$. From the plots in Figure (3.10), we observe that the experimentally measured values of $R(D)$, $R(D^*)$, and $R(X_c)$ can be achieved in two distinct parameter space regions for δm : one in the range of a few GeV to several tens of GeV ($2 < \delta m < 40$ GeV) and another in the TeV range ($\delta m < 2$ TeV or $\delta m < 5$ TeV). From the plot on the left panel of Figure (3.10), we obtain an upper limit on the mass of the exotic quark, $m_{U_1} < 4$ TeV. We illustrate the allowed parameter space consistent with experimental values in the $\delta m - m_{U_1}$ plane in Figure (3.11). The parameter δm is constrained by the experimental values of these ratios and by the mass hierarchy of the new leptons and quarks, as shown in Figure (3.11). For all scenarios ($E_i U_i$, $E_n U_n$, $E_i U_n$, $E_n U_i$), the correction δm reaches values at both the electroweak and TeV energy scales. The

allowed parameter space depends on the mass hierarchy of the exotic quarks. For the cases $E_i U_n$ and $E_n U_n$, the parameter space of δm is limited to a few GeV to several tens of GeV. The allowed TeV energy range is constrained by a curved boundary, imposing an upper limit on the mass of the exotic quarks. For the cases $E_i U_i$ and $E_n U_i$, the parameter space of δm reaches either a few GeV or a few TeV. The allowed TeV-scale energy region is a portion of the plane, bounded by lines where δm remains constant in the $\delta m - m_{U_1}$ plane. This corresponds to the absence of an upper bound on the mass of the exotic quarks. The above predictions strongly depend on δm and the mass hierarchy of the new leptons and quarks.

3.3.4. Investigating Some Observations Related to Flavor Non-Universality in Interactions

Transition $s \rightarrow u$

We consider the ratios:

$$\frac{\Gamma(K \rightarrow \mu\bar{\nu})}{\Gamma(K \rightarrow e\bar{\nu})}, \quad \frac{\Gamma(\tau \rightarrow K\nu)}{\Gamma(K \rightarrow e\bar{\nu})}, \quad \frac{\Gamma(K^+ \rightarrow \pi^0\bar{\mu}\nu)}{\Gamma(K^+ \rightarrow \pi^0\bar{e}\nu)}$$

in the MF331 model. We obtain:

$$\begin{aligned} \frac{\Gamma(K \rightarrow \mu\bar{\nu})}{\Gamma(K \rightarrow e\bar{\nu})} &= \frac{\sum_k |C_{2k}^{us}|^2}{\sum_k |C_{1k}^{us}|^2} \times \left[\frac{\sum_k |C_{1k}^{us}|^2}{\sum_k |C_{2k}^{us}|^2} \right]_{SM} \times \left[\frac{\Gamma(K \rightarrow \mu\bar{\nu})}{\Gamma(K \rightarrow e\bar{\nu})} \right]_{SM}, \\ \frac{\Gamma(\tau \rightarrow K\nu)}{\Gamma(K \rightarrow e\bar{\nu})} &= \frac{\sum_k |C_{3k}^{us}|^2}{\sum_k |C_{1k}^{us}|^2} \times \left[\frac{\sum_k |C_{1k}^{us}|^2}{\sum_k |C_{3k}^{us}|^2} \right]_{SM} \times \left[\frac{\Gamma(\tau \rightarrow K\nu)}{\Gamma(K \rightarrow e\bar{\nu})} \right]_{SM}, \\ \frac{\Gamma(K^+ \rightarrow \pi^0\bar{\mu}\nu)}{\Gamma(K^+ \rightarrow \pi^0\bar{e}\nu)} &= \frac{\sum_k |C_{2k}^{us}|^2}{\sum_k |C_{1k}^{us}|^2} \times \left[\frac{\sum_k |C_{1k}^{us}|^2}{\sum_k |C_{2k}^{us}|^2} \right]_{SM} \times \left[\frac{\Gamma(K^+ \rightarrow \pi^0\bar{\mu}\nu)}{\Gamma(K^+ \rightarrow \pi^0\bar{e}\nu)} \right]_{SM}. \end{aligned}$$

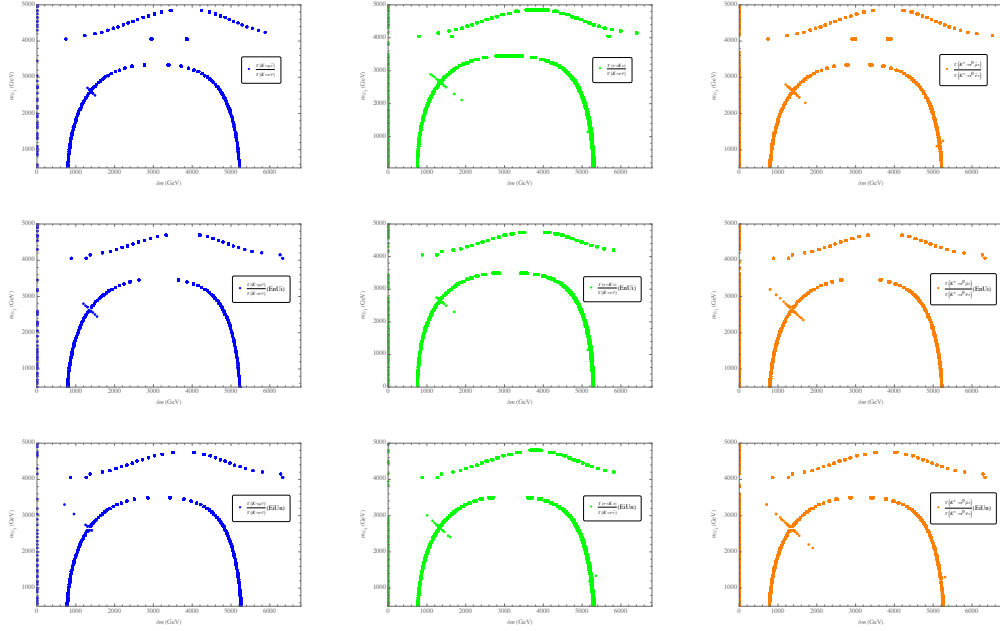
The experimental values for these ratios are given:

$$\left[\frac{\Gamma(K \rightarrow \mu\bar{\nu})}{\Gamma(K \rightarrow e\bar{\nu})} \right]_{exp} = 4.018(3) \times 10^4; \left[\frac{\Gamma(\tau \rightarrow K\nu)}{\Gamma(K \rightarrow e\bar{\nu})} \right]_{exp} = 1.89(3) \times 10^7; \left[\frac{\Gamma(K^+ \rightarrow \pi^0\bar{\mu}\nu)}{\Gamma(K^+ \rightarrow \pi^0\bar{e}\nu)} \right]_{exp} = 0.660(3) \quad (3.20)$$

as well as the values predicted by the SM:

$$\left[\frac{\Gamma(K \rightarrow \mu\bar{\nu})}{\Gamma(K \rightarrow e\bar{\nu})} \right]_{SM} = 4.0037(2) \times 10^4; \left[\frac{\Gamma(\tau \rightarrow K\nu)}{\Gamma(K \rightarrow e\bar{\nu})} \right]_{SM} = 1.939(4) \times 10^7; \left[\frac{\Gamma(K^+ \rightarrow \pi^0\bar{\mu}\nu)}{\Gamma(K^+ \rightarrow \pi^0\bar{e}\nu)} \right]_{SM} = 0.663(2) \quad (3.21)$$

In all three cases, the allowed parameter space for δm , which can explain these experimental values, is also divided into either the electroweak scale or the TeV scale. The allowed parameter space regions are determined by their consistency with the experimental values of $R(D)$, $R(D^{(*)})$, and $R(X_c)$ as previously analyzed.



Hình 3.12:

Transition $d \rightarrow u$. Experimental values for these decay ratios are:

$$\left[\frac{\Gamma(\tau \rightarrow \pi\nu)}{\Gamma(\pi \rightarrow e\bar{\nu})} \right]_{\text{exp}} = 7.90(5) \times 10^7, \quad \left[\frac{\Gamma(\pi \rightarrow \mu\bar{\nu})}{\Gamma(\pi \rightarrow e\bar{\nu})} \right]_{\text{exp}} = 8.13(3) \times 10^3. \quad (3.22)$$

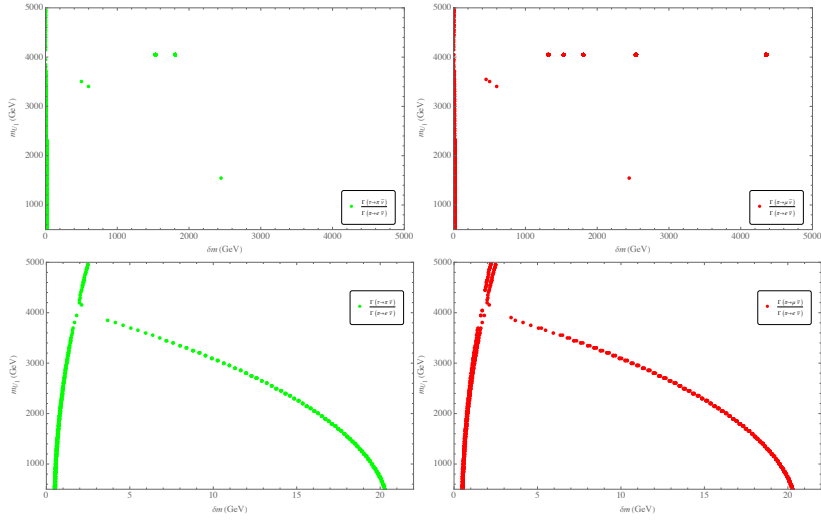
Meanwhile, the predictions from the Standard Model (SM) are:

$$\left[\frac{\Gamma(\tau \rightarrow \pi\nu)}{\Gamma(\pi \rightarrow e\bar{\nu})} \right]_{\text{SM}} = 7.91(1) \times 10^7, \quad \left[\frac{\Gamma(\pi \rightarrow \mu\bar{\nu})}{\Gamma(\pi \rightarrow e\bar{\nu})} \right]_{\text{SM}} = 8.096(1) \times 10^3. \quad (3.23)$$

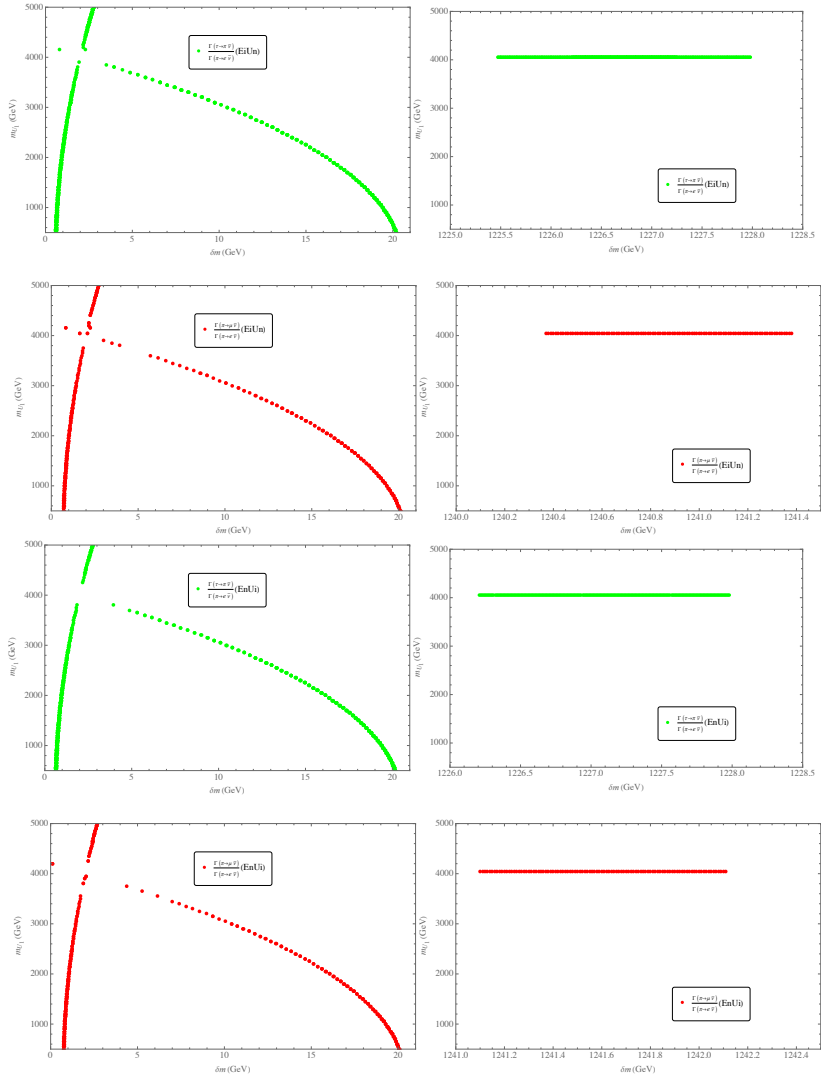
The MF331 model predicts the following expressions:

$$\begin{aligned} \frac{\Gamma(\pi \rightarrow \mu\bar{\nu})}{\Gamma(\pi \rightarrow e\bar{\nu})} &= \frac{\sum_k |C_{2k}^{ud}|^2}{\sum_k |C_{1k}^{ud}|^2} \times \left[\frac{\sum_k |C_{1k}^{ud}|^2}{\sum_k |C_{2k}^{ud}|^2} \right]_{\text{SM}} \times \left[\frac{\Gamma(\pi \rightarrow \mu\bar{\nu})}{\Gamma(\pi \rightarrow e\bar{\nu})} \right]_{\text{SM}}, \\ \frac{\Gamma(\tau \rightarrow \pi\nu)}{\Gamma(\pi \rightarrow e\bar{\nu})} &= \frac{\sum_k |C_{1k}^{ud}|^2}{\sum_k |C_{1k}^{ud}|^2} \times \left[\frac{\sum_k |C_{1k}^{ud}|^2}{\sum_k |C_{3k}^{ud}|^2} \right]_{\text{SM}} \times \left[\frac{\Gamma(\tau \rightarrow \pi\nu)}{\Gamma(\pi \rightarrow e\bar{\nu})} \right]_{\text{SM}}. \end{aligned} \quad (3.24)$$

In Figures (3.13), (3.14), we plot the contour lines for the ratios $\frac{\Gamma(\tau \rightarrow \pi\nu)}{\Gamma(\pi \rightarrow e\bar{\nu})}$ and $\frac{\Gamma(\pi \rightarrow \mu\bar{\nu})}{\Gamma(\pi \rightarrow e\bar{\nu})}$ as functions of m_{U_1} and δm in the possible cases considered in the previous sections. For the case where $m_{E_1} = m_{E_2} = m_{E_3}$ and $m_{U_1} = m_{U_2} = m_{U_3}$, we find that in the TeV-scale region, there exist certain values of δm that predict these ratios to be consistent with experimental values. Meanwhile, the GeV region of δm is predicted to explain these values. In the range $2 \text{ GeV} < \delta m < 20 \text{ GeV}$, the upper bound on m_{U_1} is less than 4 TeV. These conclusions also apply to the cases $E_d U_n$ and $E_n U_d$.



Hình 3.13:



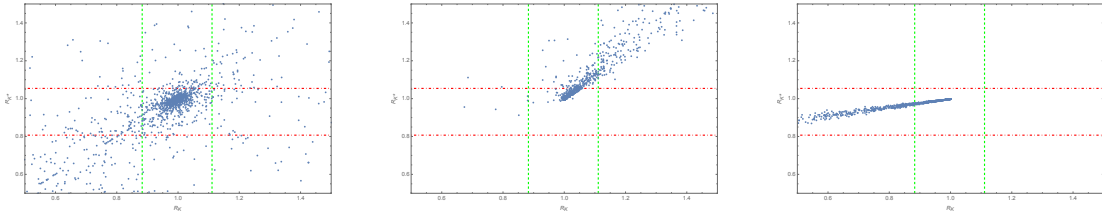
Hình 3.14:

Let us consider the allowed parameter space obtained from studying the transition

processes $b - c, s - u, d - u$. The parameter space in the first case, where $m_{E_1} = m_{E_2} = m_{E_3}$ and $m_{U_1} = m_{U_2} = m_{U_3}$, is determined by the intersection of the $m_{U_1} - \delta m$ planes shown in Figures (3.10), (3.12), and (3.13). We conclude that the allowed region is a part of the plane bounded by δm and m_{U_1} as follows: $2 < \delta m < 20$ GeV, $m_{U_1} < 4$ TeV, or $\delta m < 2$ TeV. The parameter space arising from the cases $E_i U_n$ and $E_n U_i$ must simultaneously be consistent with the values described in Figures (3.11) and (3.14). Specifically, when δm is at the GeV energy scale, there is no common set of $m_{U_1} - \delta m$ values. However, at the TeV energy scale, there exists a narrow region of $m_{U_1} - \delta m$ that is compatible with the experimental values of lepton flavor universality observables. In summary, the above predictions strongly depend on the mass splitting δm and the hierarchical structure of the masses of the new leptons and new quarks.

3.4. Analysis of the Ratios R_K, R_{K^*} Based on New Experimental Data from 2022

In December 2022, an updated LHCb analysis of R_K and R_{K^*} based on the complete Run 1 and 2 datasets was presented. These new results are consistent with SM predictions. Based on this, the authors conducted a reassessment of New Physics (NP) effects in the R_K and R_{K^*} ratios within the MF331 model framework. Through random parameter scanning in the ranges $\delta m \in [2, 20]$ GeV and $m_{U_1} \in [200, 5000]$ GeV, three mass hierarchy scenarios were examined: (i) homogeneous new fermion masses $m_{E_1} = m_{E_2} = m_{E_3}, m_{U_1} = m_{U_2} = m_{U_3}$, (ii) mixing states of type $E_i U_n$, and (iii) mixing states of type $E_n U_i$. Results indicate that in the first two scenarios, the model can effectively predict R_K and R_{K^*} values consistent with recent experimental data, with the $EiUn$ scenario showing the highest degree of compatibility. Conversely, the $EnUi$ scenario generates a nearly linear point distribution and not only reproduces the new data but also encompasses pre-2022 results, although the relevant parameter spaces exhibit distinct differences. This demonstrates that the MF331 model maintains the capacity to reasonably describe B-meson decay anomalies under appropriate parameter configurations.



Hình 3.15:

CONCLUSION AND RECOMMENDATIONS

1. The dissertation has approached the latest experimental results related to recent anomalies, specifically those associated with lepton flavor universality violation in weak interaction currents. The anomaly associated with charged currents is observed in the decay channel $b \rightarrow c\ell^-\bar{\nu}_\ell$. This decay channel is predicted in the Standard Model (SM) at the tree level approximation. However, recent experimental results indicate a significant discrepancy compared to SM predictions. Specifically, the experimentally measured values of R_D and R_{D^*} are over 25% larger than the SM predictions. Moreover, in a 2014 experiment at the LHC, the research group led by R. Aaij published findings in Physical Review Letters related to the violation of lepton flavor universality in the decay channel $b \rightarrow s\ell^+\ell^-$, within the invariant mass-squared range of the outgoing leptons ($1.0 \leq q^2 \leq 6.0 \text{ GeV}^2$). This decay channel is predicted to exist in the SM through loop-level contributions. However, the experimental results measured: $R_K^{\text{LHCb}} ([1.1, 6] \text{ GeV}^2) = 0.745^{+0.090}_{-0.074} \pm 0.036$, while the SM predicts $R(K) \simeq 1$. Our research group, based on these experimental results, has explored new physics models in search of explanations for lepton flavor universality violation. In addition to studies conducted by the theoretical physics research community, we have identified that a possible solution to these anomalies could stem from extending the particle spectrum by introducing scalar leptoquarks. However, leptoquark-based models may face stringent constraints from proton decay processes.

At this point, we have identified that constructing a physical model in which lepton number universality is inherently violated could provide a strong theoretical explanation for these experimental results. We have discovered that the F331 model is a relatively simple framework for lepton flavor universality violation. In the MF331 model, the first-generation leptons transform as a sextet, while the other two generations transform as a triplet under the $SU(3)_L$ transformation. All three generations of quarks transform as an anti-triplet under $SU(3)_L$. With this arrangement, we observe that:

- The existence of interactions between leptons and gauge bosons leads to a violation of lepton flavor universality.
- The first-generation leptons possess new interactions that are absent in the other two generations.
- All three generations of quarks transform identically, ensuring quark flavor uni-

versality at the tree-level approximation. No tree-level flavor-changing neutral currents exist.

Based on the characteristics of lepton flavor universality-violating interactions mentioned above, we investigate flavor-changing processes associated with the neutral current transition $b \rightarrow s\ell^+\ell^-$ and subsequently calculate their contributions to the ratios R_K and R_{K^*} . We conduct a numerical analysis to explain the experimental data on R_K and R_{K^*} published by the LHC in 2014. The results indicate that the ratios R_K and R_{K^*} can only be explained if the model allows for mass degeneracy between the new leptons appearing in the sextet of the first-generation leptons and the new quarks. In the absence of this degeneracy, the model predicts negligible new contributions, meaning that the ratios $R_K, R_{K^*} \simeq 1$, similar to the Standard Model predictions.

2. In addition to anomalies arising from neutral currents, we further explore the contributions of new physics to charged currents. The new physics contributions to the observables R_D and R_{D^*} are strongly dependent on the mass splitting parameter $\delta m = m_{\xi^\pm} - m_{E_1} = m_{E_1} - m_{\xi^0}$. We find that when δm is on the order of several tens of GeV or around the TeV scale, the model successfully explains the experimental values of R_D and R_{D^*} .

Based on the parameter space that explains R_D and R_{D^*} , we further investigate and evaluate processes related to R_{X_c} as well as flavor-changing transitions such as $s \rightarrow u$ and $d \rightarrow u$. Our predictions for these processes are found to be fully consistent with experimental data. Furthermore, if the parameter space explaining the experimental results for R_D , R_{D^*} , and R_{X_c} , as well as for the transitions $s \rightarrow u$ and $d \rightarrow u$, requires a mass separation between the new leptons and new quarks, then the model cannot explain the 2014 measurements of R_K and R_{K^*} . However, in December 2022, LHCb reanalyzed the experimental data using the full Run 1 and Run 2 datasets, revealing that the ratios were consistent with $R_K \simeq 1$ and $R_{K^*} \simeq 1$. Consequently, we revisited our analysis and found that when the mass splitting δm is of the order of several tens of GeV or around the TeV scale, the predicted values of R_K and R_{K^*} in our model approach 1, aligning with the updated experimental results.

3. We also discuss the potential for discovering new physics (NP) at accelerators such as the LHC and LEP. The LEPII experiment has searched for a neutral boson Z' , setting a lower mass limit of 1.13 TeV, while constraints from meson mixing push this limit above 4 TeV in the 331 model. At the LHC, heavy exotic quarks and leptons can be produced through gluon-gluon interactions and the Drell-Yan mechanism. Due to small mass differences, the exotic leptons exhibit unique decay modes, including decays into Standard Model particles such as leptons, and the bosons W and Z . Notably, the exotic leptons ξ^0 and ξ^\pm carry zero lepton number, leading to certain decay processes that violate lepton number conservation. Additionally, heavy neutral scalars H' can be efficiently produced at the LHC via mechanisms involving heavy exotic quarks, with significantly higher production rates compared to traditional Higgs models.

LIST OF PUBLICATIONS RELATED TO THE DISSERTATION

1. P. N. Thu , N. T. Duy, A E Cárcamo Hernández, D. T. Huong, *Lepton universality violation in the minimal flipped 331 model*, Progress of Theoretical and Experimental Physics **12**, 123B01, 2023.
2. N. T. Duy, P. N. Thu, D. T. Huong, *New physics in $b \rightarrow s$ transitions the MF331 model*, European Physical Journal C **82**, 966, 2022.

TÀI LIỆU THAM KHẢO

- [1] C. Patrignani *et al.* (Particle Data Group), 2016, *Chin. Phys. C*, 40, 100001.
- [2] G. Aad *et al.* (ATLAS Collaboration), 2012, Observation of a new particle in the search for the Standard Model Higgs boson with the ATLAS detector at the LHC, *Phys. Lett. B*, 716, 1-29.
- [3] S. Chatrchyan *et al.* (CMS Collaboration), 2012, Observation of a new boson at a mass of 125 GeV with the CMS experiment at the LHC, *Phys. Lett. B*, 716, 30-61.
- [4] G. Bellini *et al.* (BOREXINO), 2014, Neutrinos from the primary proton–proton fusion process in the Sun, *Nature*, 512, no.7515, 383-386.
- [5] B. T. Cleveland, T. Daily, R. Davis, Jr., J. R. Distel, K. Lande, C. K. Lee, P. S. Wildenhain and J. Ullman, 1998, Measurement of the solar electron neutrino flux with the Homestake chlorine detector, *Astrophys. J.*, 496, 505-526.
- [6] F. Kaether, W. Hampel, G. Heusser, J. Kiko and T. Kirsten, 2010, Reanalysis of the GALLEX solar neutrino flux and source experiments, *Phys. Lett. B*, 685, 47-54.
- [7] J. N. Abdurashitov *et al.* (SAGE), 2009, Measurement of the solar neutrino capture rate with gallium metal. III: Results for the 2002- 2007 data-taking period, *Phys. Rev. C*, 80, 015807.
- [8] K. Abe *et al.* (Super-Kamiokande), 2011, Solar neutrino results in Super-Kamiokande-III, *Phys. Rev. D*, 83, 052010.
- [9] B. Aharmim *et al.* (SNO), 2013, Combined analysis of all three phases of solar neutrino data from the Sudbury Neutrino Observatory , *Phys. Rev. C*, 88, 025501.
- [10] G. Bellini, J. Benziger, D. Bick, S. Bonetti, G. Bonfini, M. Buizza Avanzini, B. Caccianiga, L. Cadonati, F. Calaprice and C. Carraro,*et al.*, 2011, Precision measurement of the ^{7}Be solar neutrino interaction rate in Borexino, *Phys. Rev. Lett.*, 107, 141302.
- [11] E. Aprile *et al.* (XENON Collaboration), First Dark Matter Search Results from the XENON1T Experiment, *Phys. Rev. Lett.*, 2017, 119, 181301.
- [12] V. A. Kuzmin, V. A. Rubakov and M. E. Shaposhnikov, 1985, On the anomalous electroweak baryon number non-conservation in the early universe, *Phys. Lett. B*, 155, 36.

- [13] G. 't Hooft, 1980, Naturalness, chiral symmetry, and spontaneous chiral symmetry breaking, *NATO Sci. Ser. B*, 59, 135-157.
- [14] , Lees, J. P. and others, BaBar, 2012 Evidence for an excess of $\bar{B} \rightarrow D^{(*)}\tau^-\bar{\nu}_\tau$ decays, 1205.5442, arXiv, hep-ex BABAR-PUB-12-012, SLAC-PUB-15028, 10.1103/PhysRevLett.109.101802, *Phys. Rev. Lett.*, 109, 101802.
- [15] Lees, J. P. and others, BaBar, 2013, Measurement of an Excess of $\bar{B} \rightarrow D^{(*)}\tau^-\bar{\nu}_\tau$ Decays and Implications for Charged Higgs Bosons, 1303.0571, arXiv, hep-ex, BABAR-PUB-13-001, SLAC-PUB-15381, 10.1103/PhysRevD.88.072012, *Phys. Rev. D*, 8, 7, 072012.
- [16] Huschle, M. and others, Belle, 2015, Measurement of the branching ratio of $\bar{B} \rightarrow D^{(*)}\tau^-\bar{\nu}_\tau$ relative to $\bar{B} \rightarrow D^{(*)}\ell^-\bar{\nu}_\ell$ decays with hadronic tagging at Bell, 1507.03233, arXiv, hep-ex, KEK-REPORT-2015-18, 10.1103/PhysRevD.92.072014, *Phys. Rev. D*, 92, 7, 072014.
- [17] Abdesselam, A. and others, Belle, 2016, *Measurement of the branching ratio of $\bar{B}^0 \rightarrow D^{*+}\tau^-\bar{\nu}_\tau$ relative to $\bar{B}^0 \rightarrow D^{*+}\ell^-\bar{\nu}_\ell$ decays with a semileptonic tagging method*, 51st Rencontres de Moriond on EW Interactions and Unified Theories, 1603.06711, arXiv, hep-ex, BELLE-CONF-160, 3.
- [18] Abdesselam, A. and others, 2016, Measurement of the τ lepton polarization in the decay $\bar{B} \rightarrow D^*\tau^-\bar{\nu}_\tau$, 608.06391, arXiv, hep-ex, 8.
- [19] Aaij, Roel and others, LHCb, 2015, Measurement of the ratio of branching fractions $\mathcal{B}(\bar{B}^0 \rightarrow D^{*+}\tau^-\bar{\nu}_\tau)/\mathcal{B}(\bar{B}^0 \rightarrow D^{*+}\mu^-\bar{\nu}_\mu)$, *Phys. Rev. Lett.*, 111, 111803.
- [20] Y. S. Amhis *et al.* (HFLAV), 2021, Averages of b-hadron, c-hadron, and τ -lepton properties as of 2018, *Eur. Phys. J. C*, 81, 22.
- [21] Bigi, Dante and Gambino, Paolo, 2016, Revisiting $B \rightarrow D\ell\nu$, 1606.08030, arXiv, hep-ph, doi = 10.1103/PhysRevD.94.094008, *Phys. Rev. D*, 94, 9, 094008.
- [22] Bernlochner, Florian U. and Ligeti, Zoltan and Papucci, Michele and Robinson, Dean J, 2017, Combined analysis of semileptonic B decays to D and D^* : $R(D^{(*)})$, $|V_{cb}|$, and new physics, 1703.05330, arXiv, hep-ph, doi = 10.1103/PhysRevD.95.115008, *Phys. Rev. D*, 95, 11, 115008. Erratum: *Phys.Rev.D* 97, 059902 (2018).
- [23] Bigi, Dante and Gambino, Paolo and Schacht, Stefan, 2017, $R(D^*)$, $|V_{cb}|$, and the Heavy Quark Symmetry relations between form factors, 1707.09509, arXiv, hep-ph, doi = 10.1007/JHEP11(2017)061, *JHEP*, 11, 06.
- [24] Jaiswal, Sneha and Nandi, Soumitra and Patra, Sunando Kumar, 2017, Extraction of $|V_{cb}|$ from $B \rightarrow D^{(*)}\ell\nu_\ell$ and the Standard Model predictions of $R(D^{(*)})$, 1707.09977, arXiv, hep-ph, doi = 10.1007/JHEP12(2017)060, *JHEP*, 12, 060.
- [25] Fajfer, Svjetlana and Kamenik, Jernej F. and Nisandzic, Ivan, 2012, On the $B \rightarrow D^*\tau\bar{\nu}_\tau$ Sensitivity to New Physics, 1203.2654, arXiv, hep-ph, doi = 10.1103/PhysRevD.85.094025, *Phys. Rev. D*, 85, 094025.

- [26] Bećirević, Damir and Košnik, Nejc and Tayduganov, Andrey, 2012 , $\bar{B} \rightarrow D\tau\bar{\nu}_\tau$ vs. $\bar{B} \rightarrow D\mu\bar{\nu}_\mu$, doi 10.1016/j.physletb.2012.08.016, *Phys. Lett. B*, 716, 208–213.
- [27] R. Aaij *et al.* (LHCb Collaboration), 2016, Measurement of the phase difference between short- and long-distance amplitudes in the $B^+ \rightarrow K^+\mu^+\mu^-$ decay, *Eur. Phys. J. C*, 77, 161.
- [28] S. Wehle *et al.* (Belle Collaboration), 2017, Lepton flavor dependent angular analysis of $B \rightarrow K^*l^+l^-$, *Phys. Rev. Lett.*, 118, 111801.
- [29] Khachatryan *et al.* (CMS Collaboration), 2016, Angular analysis of the decay $B \rightarrow K^*\mu^+\mu^-$ from pp collisions at $\sqrt{s} = 8$ TeV, *Phys. Lett. B*, 753, 424.
- [30] A. M. Sirunyan *et al.* (CMS Collaboration), 2018, Measurement of angular parameters from the decay $B^0 \rightarrow K^{*0}\mu^+\mu^-$ decay in proton-proton collisions at $\sqrt{s} = 8$ TeV, *Phys. Rev. D*, 98, 112011.
- [31] R. Aaij *et al.* (LHCb Collaboration), 2014, Differential branching fractions and isospin asymmetries of $B \rightarrow K^{(*)}\mu^+\mu^-$ decays, *JHEP*, 06, 133.
- [32] R. Aaij *et al.* (LHCb Collaboration), 2021, Branching fraction measurements of the rare $B_s^0 \rightarrow \phi\mu^+\mu^-$ and $B_s^0 \rightarrow f'_2(1525)\mu^+\mu^-$ decays, *Phys. Rev. Lett.*, 127, 151801.
- [33] R. Aaij *et al.* (LHCb Collaboration), 2013, Measurement of form-factor-independent observables in the decay $B^0 \rightarrow K^{0*}\mu^+\mu^-$, *Phys. Rev. Lett.*, 111, 191801.
- [34] R. Aaij *et al.* (LHCb Collaboration), 2016, Angular analysis of the $B^0 \rightarrow K^{0*}\mu^+\mu^-$ decay using $3 fb^{-1}$ of integrated luminosity, *JHEP*, 02, 104.
- [35] R. Aaij *et al.* (LHCb Collaboration), 2015, Angular analysis of the decay $B \rightarrow K^{*0}e^+e^-$ decay in low- q^2 region, *JHEP*, 04, 064.
- [36] M. Aaboud *et al.* (ATLAS Collaboration), Angular analysis of $B_d^0 \rightarrow K^*\mu^+\mu^-$ decay in pp collisions at $\sqrt{s} = 8$ TeV with the ATLAS detector, *JHEP*, 10, 047.
- [37] R. Aaij *et al.* (LHCb Collaboration), 2020, Measurement of CP -averaged observables in the $B^0 \rightarrow K^{*0}\mu^+\mu^-$ decay, *Phys. Rev. Lett.*, 125, 011802.
- [38] R. Aaij *et al.* (LHCb Collaboration), 2021, Angular analysis of the decay $B^+ \rightarrow K^{*+}\mu^+\mu^-$, *Phys. Rev. Lett.*, 126, 161802.
- [39] R. Aaij *et al.* (LHCb Collaboration), 2017, Test of lepton universality with $B^0 \rightarrow K^{*0}l^+l^-$ decays, *JHEP*, 08, 55.
- [40] S. Wehle *et al.* (Belle Collaboration), 2021, Test of lepton universality using $B^+ \rightarrow K^+l^+l^-$ decays at Belle, *Phys. Rev. Lett.*, 126, 161801.
- [41] R. Aaij *et al.* (LHCb Collaboration), 2022, Test of lepton universality in beauty-quark decays, *Nature Phys.*, 18, 277-282.

- [42] R. Aaij *et al.* (LHCb Collaboration), 2014, Test of lepton universality using $B^+ \rightarrow K^+ l^+ l^-$ decays, *Phys. Rev. Lett.*, 113, 151601.
- [43] R. Aaij *et al.* (LHCb Collaboration), 2019, Search for lepton-universality violation in $B^+ \rightarrow K^+ l^+ l^-$, *Phys. Rev. Lett.*, 122, 191801.
- [44] M. Bordone, G. Isidori and A. Patti, 2016, the Standard Model predictions for R_K and R_{K^*} , *Eur. Phys. J. C*, 76, 440.
- [45] B. Capdevila, A. Crivellin, S. Descotes-Genon, J. Matias and J. Virto, 2018, Patterns of New Physics in $b \rightarrow sl^+l^-$ transitions in the light of recent data, *JHEP*, 01, 093.
- [46] P. Van Dong, N. T. K. Ngan, T. D. Tham, L. D. Thien, N. T. Thuy, 2019, Phenomenology of the simple 3-3-1 model with inert scalars, *Phys. Rev. D*, 99, 095031.
- [47] P. V. Dong, D. T. Huong, F. S. Queiroz, and N. T. Thuy, 2014, Phenomenology of the 3-3-1-1 model, *Phys. Rev. D*, 90, 075021.
- [48] R. M. Fonseca and M. Hirsch, 2016, A flipped 331 model, *JHEP* 08, 003.
- [49] Van Loi, Duong and Van Dong, Phung and Van Soa, Dang, 2020, Neutrino mass and dark matter from an approximate B – L symmetry, *JHEP*, 090, 5, 2020.
- [50] T Morii (Kobe University, Japan), C S Lim (Kobe University, Japan), and S N Mukherjee (Banaras Hindu University, India), 2004, The Physics of the Standard Model and Beyond, <https://doi.org/10.1142/4655>
- [51] Roos và Sirlin, 1971, *Nucl. Phys. B*, 29, 296-304; M. A. Beg and A. Sirlin, 1982, *Phys. Rep.*, 88, 1.
- [52] The Particle Data Group, C. Patrignani *et al.*, 2016, Review of particle physics, *Chin. Phys. C40* (2016) 100001, and 2017 update.
- [53] Particle Data Group, 2002, *Phys. Rev. D* 66, 010001
- [54] Braun *et al.*, 1975, A Study of the Semileptonic Decays of K+ Mesons, *Nucl.Phys.B*, 89, 210-252.
- [55] Bourquin et al., 1983, Measurements of Hyperon Semileptonic Decays at the CERN Super Proton Synchrotron, *Z.Phys.C* 21, 1. <https://doi.org/10.1007/BF01648771>
- [56] The ALEPH, DELPHI, L3, OPAL, SLD Collaborations, the LEP Electroweak Working Group, the SLD Electroweak and Heavy Flavour Groups, 2006, Precision Electroweak Measurements on the Z Resonance, *Phys. Rept.*, 427, 257, arXiv:hep-ex/0509008.
- [57] DELPHI, OPAL, LEP Electroweak, ALEPH, L3, S. Schael et al., 2013, Electroweak Measurements in Electron-Positron Collisions at W-Boson-Pair Energies at LEP, *Phys. Rept.*, 532, 119, arXiv:1302.3415.
- [58] V. Cirigliano and I. Rosell, 2007, Two-Loop Effective Theory Analysis of $\pi(K) \rightarrow e\bar{\nu}_e[\gamma]$ Branching Ratios, *Phys. Rev. Lett.*, 99, 231801, arXiv:0707.3439.

- [59] NA62 collaboration, C. Lazzeroni et al., 2013, Precision Measurement of the Ratio of the Charged Kaon Leptonic Decay Rates, *Phys. Lett. B*, 719, 326, arXiv:1212.4012.
- [60] PiENu, A. Aguilar-Arevalo et al., 2015, Improved Measurement of the $\pi \rightarrow e\nu$ Branching Ratio, *Phys. Rev. Lett.*, 115, no. 7 071801, arXiv:1506.05845.
- [61] HFLAV collaboration, Y. Amhis et al., Averages of b-hadron, c-hadron, and τ -lepton properties as of summer 2016, *Eur. Phys. J. C*, 77, 895, arXiv:1612.07233.
- [62] B. A. Dobrescu and A. S. Kronfeld, 2008, Accumulating evidence for nonstandard leptonic decays of Ds mesons, *Phys. Rev. Lett.*, 100, 241802, arXiv:0803.0512.
- [63] MILC collaboration, J. A. Bailey et al., 2015, $B \rightarrow D\ell\nu$ form factors at nonzero recoil and $|V_{cb}|$ from 2+1-flavor lattice QCD, *Phys. Rev. D*, 92, 034506, arXiv:1503.07237.
- [64] HPQCD collaboration, H. Na *et al.*, 2015, $B \rightarrow D\ell\nu$ form factors at nonzero recoil and extraction of $|V_{cb}|$, *Phys. Rev. D*, 92, 054510, arXiv:1505.03925, [Erratum: *Phys. Rev.D*93,119906(2016)].
- [65] A. Crivellin, C. Greub, and A. Kokulu, *Phys. Rev. D*, 86, 054014. [arXiv:1206.2634[hep-ph]]. <https://doi.org/10.1103/PhysRevD.86.054014>.
- [66] A. Celis, M. Jung, X.-Q. Li, and A. Pich, 2013, *J. High Energy Phys.*, 1301, 054. [arXiv:1210.8443[hep-ph]]. [https://doi.org/10.1007/JHEP01\(2013\)054](https://doi.org/10.1007/JHEP01(2013)054).
- [67] A. Crivellin, A. Kokulu, and C. Greub, 2013, *Phys. Rev. D*, 87, 094031. [arXiv:1303.5877[hep-ph]]. <https://doi.org/10.1103/PhysRevD.87.094031>.
- [68] A. Greljo, G. Isidori, and D. Marzocca, 2015, *J. High Energy Phys.*, 1507, 142. [arXiv:1506.01705[hep-ph]]. [https://doi.org/10.1007/JHEP07\(2015\)142](https://doi.org/10.1007/JHEP07(2015)142).
- [69] S. M. Boucenna, A. Celis, J. Fuentes-Martin, A. Vicente, and J. Virto, 2016, *J. High Energy Phys.*, 1612, 059. [arXiv:1608.01349[hep-ph]]. [https://doi.org/10.1007/JHEP12\(2016\)059](https://doi.org/10.1007/JHEP12(2016)059).
- [70] I. Doršner, S. Fajfer, A. Greljo, J. F. Kamenik, and N. Košnik, 2016, *Phys. Rept.*, 641, 1. [arXiv:1603.04993[hep-ph]]. <https://doi.org/10.1016/j.physrep.2016.06.001>.
- [71] M. Bauer and M. Neubert, 2016, *Phys. Rev. Lett.*, 116, 141802. [arXiv:1511.01900[hep-ph]]. <https://doi.org/10.1103/PhysRevLett.116.141802>.
- [72] S. Fajfer and N. Košnik, *Phys. Lett. B*, 755, 270. [arXiv:1511.06024[hep-ph]]. <https://doi.org/10.1016/j.physletb.2016.02.018>.
- [73] R. Barbieri, G. Isidori, A. Pattori, and F. Senia, 2016, *Eur. Phys. J. C*, 76, 67. [arXiv:1512.01560[hep-ph]]. <https://doi.org/10.1140/epjc/s10052-016-3905-3>.
- [74] D. Bećirević, S. Fajfer, N. Košnik, and O. Sumensari, *Phys. Rev. D*, 94, 115021. [arXiv:1608.08501[hep-ph]]. <https://doi.org/10.1103/PhysRevD.94.115021>.

- [75] G. Hiller, D. Loose, and K. Schönwald, 2016, *J. High Energy Phys.*, 1612, 027. [arXiv:1609.08895[hep-ph]]. [https://doi.org/10.1007/JHEP12\(2016\)027](https://doi.org/10.1007/JHEP12(2016)027).
- [76] A. Crivellin, D. Müller, and T. Ota, 2017, *J. High Energy Phys.*, 1709, 040. [arXiv:1703.09226[hep-ph]]. [https://doi.org/10.1007/JHEP09\(2017\)040](https://doi.org/10.1007/JHEP09(2017)040). Downloaded from <https://academic.oup.com/ptep/article/2023/12/123B01/7382242> by guest on 13 December 2023.
- [77] A. Abada, A. M. Teixeira, A. Vicente, and C. Weiland, 2014, *J. High Energy Phys.*, 1402, 091. [arXiv:1311.2830[hep-ph]]. [https://doi.org/10.1007/JHEP02\(2014\)091](https://doi.org/10.1007/JHEP02(2014)091).
- [78] G. Cvetic and C. S. Kim, 2017, *Phys. Rev. D*, 94, 053001 (2016); 95, 039901. [erratum][arXiv:1606.04140[hep-ph]]. . <https://doi.org/10.1103/PhysRevD.94.053001>.
- [79] L.-S. Geng et al., 2017, Towards the discovery of new physics with lepton-universality ratios of $b \rightarrow s\ell\ell$ decays, *Phys. Rev. D*, 96, 093006, arXiv:1704.05446.
- [80] W. Altmannshofer, C. Niehoff, P. Stangl, and D. M. Straub, 2017, Status of the $b \rightarrow K^*\mu^+\mu^-$ anomaly after Moriond 2017, *Eur. Phys. J. C*, 77, 377, arXiv:1703.09189.
- [81] Choudhury, S., Sandilya, S. et al., (Belle), 2021, Test of lepton flavor universality and search for lepton flavor violation in $B \rightarrow Kl^+l^-$ decays, *JHEP*, 3, 105.
- [82] Hiller, Gudrun and Kruger, Frank, 2014, More Model-Independent Analysis of $b \rightarrow s$ Processes, *Phys. Rev. D*, 79, 074020.
- [83] Hiller, Gudrun and Kruger, Frank, 2015, Diagnosing lepton-nonuniverality $b \rightarrow s\ell\ell$, *JHEP*, 2, 055.
- [84] Altmannshofer, Wolfgang and Stangl, Peter and Straub, David M, 2017, Interpreting hints for lepton flavor universality violation , *Phys. Rev. D*, 96, 055008.
- [85] Arbey, A. and Hurth, T. and Mahmoudi, F. and Martínez Santos, D. and Neshatpour, S, 2019, Update on the $b \rightarrow s$ anomalies, *Phys. Rev. D*, 100, 015045.
- [86] Arbey, A. and Hurth, T. and Mahmoudi, F. and Martínez Santos, D. and Neshatpour, S, 2019, Continuing search for new physics in $b \rightarrow s\mu^+\mu^-$ decays: two operators at a time , *JHEP*, 06, 089.
- [87] Wolfgang Altmannshofer and Peter Stangl, 2021, New physics in rare B decays after Moriond 2021, *JHEP*, arXiv: 2103.13370.
- [88] T. Hurth, F. Mahmoudi, D. Martinez Santos, S. Neshatpour, 2014, More indications for lepton nonuniversality $b \rightarrow sl^+l^-$, *JHEP*, arXiv: 2104.10058
- [89] Allanach, Ben and QueiroZ, Farinaldo S. and Strmia, Alessandro and Sun, Sichun, 2016, Z' models for the LHCb and $g - 2$ muon anomalies, *Phys. Rev. D*, 93, 055045.
- [90] Altmannshofer, Wolfgang and Gori, Stefania and Profumo, Stefano and Queiro, Farinaldo S, 2016, Explaining dark matter and B decay anomalies with an L_μ - L_τ model, *JHEP*, 12, 106.

- [91] Altmannshofer, Ben Gripaios, Marco Nardecchia, S. A. Renner, 2015, Composite leptons and anomalies in B -meson decays, *JHEP*, 05,065.
- [92] S. Fajfer and N. Konik, 2016, Vector leptoquark resolution of R_K and R_{D^*} puzzles, *Phys. Lett. B*, 10, 270.
- [93] L. collaboration, 2022, Test of lepton universality in $b \rightarrow s l^+ l^-$ decays.
- [94] L. collaboration, 2022, Measurement of lepton universality parameters in $b \rightarrow k \ell^+ \ell^-$ and $b^0 \rightarrow k^{0*} \ell^+ \ell^-$ decays.
- [95] M. Gell-Mann, P. Ramond, and R. Slansky, in Supergravity, edited by P. van Nieuwenhuizen and D. Z. Freedman, North-Holland, Amsterdam, (1979), 315; T. Yanagida, edited by O. Sawada and A. Sugamoto KEK Report No. 79-18, Tsukuba, Japan, 1979), p. 95; R. N. Mohapatra and G. Senjanovic, *Phys. Rev. Lett.* 44, 912(1980).
- [96] H. Ishimori, T. Kobayashi, H. Ohki, Y. Shimizu, H. Okada, and M. Tanimoto, *Prog. Theor. Phys. Suppl.* 183 (2010), 1; G. Altarelli and F. Feruglio, *Rev. Mod. Phys.* 82, (2010), 2701; E. Ma and G. Rajasekaran, *Phys. Rev. D* 64, (2001), 113012; E. Ma, *Mod. Phys. Lett. A* 17, (2002), 289; K. S. Babu, E. Ma, and J. W. F. Valle, *Phys. Lett. B* 552, (2003) 207; P. Q. Hung and T. Le, *JHEP* 1509, (2015) 001, [*JHEP* 1509, (2015),134]; Nguyen Anh Ky, Phi Quang Van and Nguyen Thi Hong Van, *Phys. Rev. D* 94, (2016), 095009.
- [97] K. Abe et al., (2017),*Phys. Rev. Lett.* 118, no. 15, 151801.
- [98] P. Coloma, M. C. Gonzalez-Garcia, M. Maltoni, and T. Schwetz, COHERENT Enlightenment of the Neutrino Dark Side, *Phys. Rev. D*, 96 no. 11, (2017) 115007; J. Liao and D. Marfatia, *Phys. Lett. B*, 775 (2017) 54–57, arXiv:1708.04255 [hep-ph]
- [99] S. K. Agarwalla, P. Bagchi, D. V. Forero, and M. Tortola, *JHEP*, 07 (2015) 06; J. Liao, D. Marfatia, and K. lores, E. A. Garces, and O. G. Miranda, *Phys. Rev. D* 98 no. 3, (2018) 035030; K. N. Deepthi, S. Goswami, and N. Nath, *Phys. Rev. D*, 96 no. 7, (2017) 075023; S. K. Agarwalla, S. S. Chatterjee, and A. Palazzo, *Phys. Lett. B*, 762 (2016) 64–71.
- [100] Refregier, A., 2003, Weak gravitational lensing by large-scale structure, *Annual Review of Astronomy and Astrophysics*, 41 (1): 645–668. arXiv:astro-ph/0307212, doi:10.1146/annurev.astro.41.111302.102207; “Quasars, lensing, and dark matter”. Physics for the 21st Century. Annenberg Foundation. 2017.; Myslewski, Rik, 2011, “Hubble snaps dark matter warping spacetime”, The Register.
- [101] Peebles, P. J. E.; Ratra, Bharat, 2003, The cosmological constant and dark energy”. *Reviews of Modern Physics.*, 75 (2): 559–606. arXiv:astro-ph/0207347. doi:10.1103/RevModPhys.75.559. S2CID 118961123.
- [102] P. Zyla et al. (Particle Data Group), 2020, Review of Particle Physics, *Prog. Theor. Exp. Phys.* 8.

- [103] M. Lisanti and J. G. Wacker, arxiv: 0704.2816, M. Cirelli, N. Fornengo and A. Strumia, *Nucl. Phys. B*, 753, (2006), 178, T. Hambye, F.-S. Ling, L. Lopez Honorez, J. Rocher, *JHEP* 0907, (2009), 090; Erratum-ibid.1005, (2010), 066.
- [104] G. Jungman, M. Kamionkowski, and K. Griest, *Phys. Reports*, 267, (1996), 195; D. Hooper and S. Profumo, *Phys.Rept.*453, (2007), 29; J. Hubisz and P. Meade, *Phys. Rev. D* 71, (2005), 035016; P. V. Dong, D. T. Huong, *Commun. Phys.* 28, (2018), 21.Whisnant, *Phys. Rev. D*, 93 no. 9, (2016) 093016; L. J. F
- [105] P. Fayet and S. Ferrara, 1977, Supersymmetry, *Phys. Rep* 32
- [106] N. Arkani-Hamed, S. Dimopoulos and G. Dvali, 1998, The Hierarchy problem and new dimensions at a millimeter, *Physics Letters*, B429, 263–272.
- [107] R. Lisa and S. Raman, 1999, A Large mass hierarchy from a small extra dimension, *Phys. Rev. Lett.*, 83, 3370–3373.
- [108] T. Appelquist, H.C. Cheng and A. D. Dobrescu, 2001, Bounds on universal extra dimensions, *Phys. Rev. D*, 64, 035002.
- [109] T. D. Lee, 1973, A Theory of Spontaneous Violation, *Phys. Rev. D*, 8, 1226.
- [110] K.S. Babu, 1988, Model of 'calculable' Majorana neutrino masses, *Phys. Lett. B*, 203, 132-136.
- [111] H. Georgi and S.L. Glashow, 1974, Unity of all elementary particle forces, *Phys. Rev. Lett*, 32 , 438–41.
- [112] H. Georgi, 1975, *Particles and Fields, Proceedings of the APS Div. of Particles and Fields*, 575.
- [113] H. Fritzsch and P. Minkowski, 1975, Unified interactions of leptons and hadrons, *Annals of Physics*, 93, 193–266.
- [114] R. N. Mohapatra and J. C. Pati, 1975, Gauge symmetry and an "isoconjugate" model of CP violation, *Phys. Rev. D*, 11, 566.
- [115] G. Senjanovic, 1979, Spontaneous breakdown of parity in a class of gauge theories, *Nucl. Phys. B*, 153, 334.
- [116] R. N. Mohapatra and G. Senjanovic, 1980, Neutrino masses and mixings in gauge models with spontaneous parity violation, *Phys. Rev. D*, 23, 165.
- [117] R. Alonso, A. Kobach, and J. Martin Camalich, 2016, New physics in the kinematic distributions of $\bar{B} \rightarrow \bar{D}^* \tau^- (\rightarrow \ell^- \bar{\nu}_\ell \nu_\tau) \bar{\nu}_\tau$, *Phys. Rev. D*, 94, 094021, arXiv:1602.07671.
- [118] Chuan-HungChen, Cheng-WeiChiang, andChun-WeiSu, 2024, Phenomenological study of a gauged $L_\mu - L_\tau$ model with a scalar leptoquark, *Phys. Rev. D*109, 055038
<https://doi.org/10.1103/PhysRevD.109.055038>

- [119] Chuan-Hung Chen, Cheng-Wei Chiang, 2024, Flavor anomalies in leptoquark model with gauged $U(1)_{L_\mu - L_\tau}$, *Phys. Rev. D* 109, 075004 <https://doi.org/10.1103/PhysRevD.109.075004>
- [120] P. V. Dong and H. N. Long, 2006, Electric charge quantization in $SU(3)_C \otimes SU(3)_L \otimes U(1)_X$ models, *Int. J. Mod. Phys. A*, 21, 6677.
- [121] M. B. Tully and G. C. Joshi, 2001, Generating neutrino mass in the 331 model, *Phys. Rev. D*, 64, 011301.
- [122] A.G. Dias, C.A.S. de Pires, and P. S. da Rodrigues Silva, 2015, Naturally light right-handed neutrinos in a 3-3-1 model, *Phys. Lett. B*, 628, 85.
- [123] D. Chang and H. N. Long, 2006, Interesting radiative patterns of neutrino mass in an $SU(3)_C \otimes SU(3)_L \otimes U(1)_X$ model with right-handed neutrinos, *Phys. Rev. D*, 73, 053006.
- [124] P. V. Dong and H. N. Long, 2008, Neutrino masses and lepton flavor violation in the 3-3-1 model with right-handed neutrinos, *Phys. Rev. D*, 77, 057302.
- [125] P. V. Dong, L. T. Hue, H. N. Long, and D. V. Soa, 2010, The 3-3-1 model with A_4 flavor symmetry, *Phys. Rev. D*, 81, 053004.
- [126] P. V. Dong, H. N. Long, D. V. Soa, and V. V. Vien, 2011, The 3-3-1 model with S_4 flavor symmetry, *Eur. Phys. J. C*, 71, 1544.
- [127] P. V. Dong, H. N. Long, C. H. Nam, and V. V. Vien, 2012, The S_3 flavor symmetry in 3-3-1 models, *Phys. Rev. D*, 85, 053001.
- [128] S. M. Boucenna, S. Morisi, and J. W. F. Valle, 2014, Radiative neutrino mass in 3-3-1 scheme, *Phys. Rev. D*, 90, 013005.
- [129] S. M. Boucenna, R. M. Fonseca, F. Gonzalez-Canales, and J. W. F. Valle, 2015, Small neutrino masses and gauge coupling unification, *Phys. Rev. D*, 91, 031702.
- [130] H. Okada, N. Okada, and Y. Orikasa, 2016, Radiative seesaw mechanism in a minimal 3-3-1 model, e *Phys. Rev. D*, 93, 073006.
- [131] C.A.S. de Pires, 2015, *Phys. Int.*, 6, 33.
- [132] P. B. Pal, 1995, The strong CP question in $SU(3)_C \otimes SU(3)_L \otimes U(1)_N$ models, *Phys. Rev. D*, 52, 1659.
- [133] A. G. Dias, C.A.S. de Pires, and P. S. R. da Silva, 2003, Discrete symmetries, invisible axion and lepton number symmetry in an economic 3 3 1 model, *Phys. Rev. D*, 68 , 115009.
- [134] A. G. Dias and V. Pleitez, 2004, Stabilizing the invisible axion in 3-3-1 models, *Phys. Rev. D*, 69, 077702.

- [135] H. N. Long and V. T. Van, 1999, Quark family discrimination and flavor changing neutral currents in the $SU(3)_C \otimes SU(3)_L \otimes U(1)$ model with right-handed neutrinos, *J. Phys. G*, 25, 2319 .
- [136] F. Pisano, 1996, A Simple solution for the flavor question, *Mod. Phys. Lett A*, 11, 2639.
- [137] A. Doff and F. Pisano, 1999, Charge quantization in the largest leptoquark bilepton chiral electroweak scheme, *Mod. Phys. Lett. A*, 14, 1133.
- [138] C.A.S. de Pires and O. P. Ravinez, 1998, Charge quantization in a chiral bilepton gauge model, *Phys. Rev. D*, 58, 035008.
- [139] C.A. S. de Pires, 1999, Remark on the vector - like nature of the electromagnetism and the electric charge quantization, *Phys. Rev. D*, 60, 075013.
- [140] P. V. Dong, N. T. K. Ngan, D.V. Soa, Simple 331 model and implication for dark matter, 2014, *Phys. Rev. D* 90, 075019.
- [141] P. V. Dong, D. T. Huong, Tr. T. Huong, H. N. Long, Fermion masses in the economical 3-3-1 model, 2006, *Phys. Rev. D* 74, 053003
- [142] J. C. Montero, F. Pisano and V. Pleitez, Neutral currents and Glashow- Iliopoulos-Maiani mechanism in $SU(3)L \otimes U(1)N$ models for electroweak interactions, *Physics Review D*, 1993, 47, 2918.
- [143] H. N. Long, $SU(3)L \otimes U(1)N$ model for right-handed neutrino neutral currents, *Physics Review D*, 1996, 54, 4691.
- [144] H.N.Long, $SU(3)L \otimes U(1)N$ modelwithright-handedneutrinos, *Physics Review D*, 1996, 53, 437.
- [145] M. Ozer, $SU(3)L \otimes U(1)X$ model of electroweak interactions without exotic quarks, *Physics Review D*, 1996, 54, 1143-1149, DOI: 10.1103/Phys- RevD.54.1143.
- [146] P. V. Dong and H. N. Long, The economical $SU(3)C \otimes SU(3)L \otimes U(1)X$ model, *Advance in High Energy Physics*, 2008, 2008, 739492.
- [147] Andrzej J. Buras, Fulvia De Fazio, Jennifer Girrbach, 2014, 331 models facing new $b \rightarrow s\mu^+\mu^-$ data, *Journal of High Energy Physics*, 02,112.
- [148] Buras, Andrzej J. and De Fazio, Fulvia and Girrbach, Jennifer and Carlucci, Maria V., 2013, The anatomy of quark flavour observables in 331 models in the flavour precision era, *JHEP*, 02,023.
- [149] Gauld, Rhorry and Goertz, Florian and Haisch, Ulrich, 2014, An explicit Z' boson explanation of the $B \rightarrow K^*\mu^+\mu^-$ anomaly, *JHEP*, 01, 069.
- [150] Buras, Andrzej J. and De Fazio, Fulvia, 2016, ε'/ε in 331 models, *JHEP*, 3, 010
- [151] D. T. Huong, D. N. Dinh, L. D. Thien, and P. Van Dong, 2019, *J. High Energy Phys.*, 051 [arXiv:1906.05240[hep-ph]]

- [152] B. Bhattacharya, A. Datta, D. London, and S. Shivashankara, 2015, *Phys. Lett. B*, 742, 370. [arXiv:1412.7164[hep-ph]]. <https://doi.org/10.1016/j.physletb.2015.02.011>.
- [153] G. Senjanovic and R. N. Mohapatra, 1975, Exact left-right symmetry and spontaneous violation of parity, *Phys. Rev. D*, 12, 1502
- [154] L. Calibbi, A. Crivellin, and T. Ota, (2015, *Phys. Rev. Lett.*, 115, 181801. [arXiv:1506.02661[hep-ph]]. <https://doi.org/10.1103/PhysRevLett.115.181801>.
- [155] Pisano, F. and Pleitez, V., 1992, SU(3) \times U(1) model for electroweak interactions puzzles, *Phys. Rev. D*, 46, 410
- [156] P. H. Frampton, 1992, Chiral dilepton model and the flavor question, *Phys. Rev. Lett.*, 69.2889
- [157] Foot, R. and Hernández, O. F. and Pisano, F. and Pleitez, V, 1993, Lepton masses in an SU(3)_L \times U(1)_N gauge model, *Phys. Rev. D*, 47.4158
- [158] Foot, R. and Hernández, O. F. and Pisano, F. and Pleitez, V, 1980, Canonical neutral-current predictions from the weak-electromagnetic gauge group SU(3) \times U(1), *Phys. Rev. D*, 47.4158
- [159] Montero, J. C. and Pisano, F. and Pleitez, V., 1993, Neutral currents and Glashow-Iliopoulos-Maiani mechanism in SU(3)_L \times U(1)_N, *Phys. Rev. D*, 47.2918
- [160] Foot, Robert and Long, Hoang Ngoc and Tran, Tuan, 1994, SU(3)_L \times U(1)_N and SU(4)_L \times U(1)_N gauge models with right-handed neutrinos, *Phys. Rev. D*, 50.R34
- [161] Du, Daping and El-Khadra, A. X. and Gottlieb, Steven and Kronfeld, A. S. and Laiho, J. and Lunghi, E. and Van de Water, R. S. and Zhou, Ran, 2016, Phenomenology of semileptonic B-meson decays with form factors from lattice QCD, *Phys. Rev. D*, 93.034005.
- [162] Beneke, Martin and Bobeth, Christoph and Szafron, Robert, 2018, Enhanced electromagnetic correction to the rare B-meson decay $B_{s,d} \rightarrow \mu^+ \mu^-$, *Phys. Rev. Lett.*, 120.011801.
- [163] L. Di Luzio, M. Nardecchia, What is the scale of new physics behind the B-flavour anomalies? *Eur. Phys. J. C* 77(8), 536 (2017). <https://doi.org/10.1140/epjc/s10052-017-5118-9>. arXiv:1706.01868 [hep-ph]
- [164] Lü, Cai-Dian and Shen, Yue-Long and Wang, Yu-Ming and Wei, Yan-Bing, 2019, QCD calculations of $B \rightarrow \pi, K$ form factors with higher-twist corrections, *JHEP* 01, 024.
- [165] Bharucha, Aoife and Straub, David M. and Zwicky, Roman, 2015, $B \rightarrow V\ell^+\ell^-$ in the Standard Model from light-cone sum rules, *JHEP*, 08,098.
- [166] Altmannshofer, Wolfgang and Straub, David M, 2015, New physics in $b \rightarrow s$ transitions after LHC run 1, *Eur. Phys. J. C*, 75, 382.

- [167] C. Bourrely, I. Caprini, and L. Lellouch, 2009, Model-independent description of $B \rightarrow \pi \ell \nu$ decays and a determination of $V(ub)$, *Phys. Rev. D*, **79** 013008, arXiv:0807.2722 [hep-ph]. [Erratum: Phys.Rev.D 82, 099902 (2010)].
- [168] Munir Bhutta, Faisal and Huang, Zhuo-Ran and Lü, Cai-Dian and Paracha, M. Ali and Wang, Wenyu, 2020, New Physics in $b \rightarrow s \ell \ell$ anomalies and its implications for the complementary neutral current decays, arXiv: 2009.03588 ICHEP2016,1.282.0554
- [169] Ali, A. Y. Parkhomenko, and A. V. Rusov, 2014, Precise Calculation of the Dilepton Invariant-Mass Spectrum and the Decay Rate in $B^\pm \rightarrow \pi^\pm \mu^+ \mu^-$ in the SM, *Phys. Rev. D*, **89** no. 9, 094021, arXiv:1312.2523 [hep-ph].
- [170] Ligeti, Zoltan and Tack- mann, Frank J., 2014, Precise predictions for $B \rightarrow X c \tau \nu$ decay distributions, *Phys. Rev. D*, **90**, 3, 034021, 7, Aug, American Physical Society, <https://link.aps.org/doi/10.1103/PhysRevD.90.034021>.
- [171] Particle Data Group, 2022, R L Workman *et al.*, *Review of Particle Physics* , Progress of Theoretical and Experimental Physics, Volume 2, Issue 8, August 2022, 083C01, <https://doi.org/10.1093/ptep/ptac097>
- [172] V. Cirigliano and I. Rosell, J. High Energy Phys. 0710, 005 (2007) [arXiv:0707.4464[hep-ph]]. <https://doi.org/10.1088/1126-6708/2007/10/005>.
- [173] V. H. Binh, D. T. Binh, A. E. Cárcamo Hernández, D. T. Huong, D. V. Soa, and H. N. Long, 2023, Higgs sector phenomenology in the 3-3-1 model with an axionlike particle, *Phys. Rev. D* **107** no. 9, 095030, arXiv:2007.05004 [hep-ph].
- [174] V. T. N. Huyen, H. N. Long, T. T. Lam, and V. Q. Phong, 2014, *Commun. Phys.* **24**, 97 [arXiv:1210.5833[hep-ph]]. <https://doi.org/10.15625/0868-3166/24/2/3774>.
- [175] A. E. Cárcamo Hernández, L. Duarte, A. S. de Jesus, S. Kovalenko, F. S. Queiroz, C. Siqueira, Y. M. Oviedo-Torres, and Y. Villamizar, 2023, *Phys. Rev. D*, **107**, 063005 [arXiv:2208.08462[hep-ph]]. <https://doi.org/10.1103/PhysRevD.107.063005>(publication).
- [176] A. E. Cárcamo Hernández, C. O. Dib, and U. J. Saldaña Salazar, 2020, *Phys. Lett. B*, **809**, 135750 [arXiv:2001.07140[hep-ph]]. <https://doi.org/10.1016/j.physletb.2020.135750>(publication). [https://doi.org/10.1007/JHEP08\(2019\)051](https://doi.org/10.1007/JHEP08(2019)051)(publication).
- [177] N. T. Duy, P. N. Thu, and D. T. Huong, 2022, New physics in $b \rightarrow s$ transitions in the MF331 model, *Eur. Phys. J. C*, **82** no. 10, 966, arXiv:2205.02995 [hep-ph].
- [178] T. Hurth, F. Mahmoudi and S. Neshatpour, Global fits to $b \rightarrow s \ell \ell$ data and signs for lepton non-universality, *JHEP* **1412**, 053 (2014) [arXiv:1410.4545 [hep-ph]].
- [179] Y. Sakaki, M. Tanaka, A. Tayduganov and R. Watanabe, Testing leptoquark models in $\bar{B} \rightarrow D^{(*)}\tau\bar{\nu}$, *Phys. Rev. D* **88**, no. 9, 094012 (2013) [arXiv:1309.0301 [hep-ph]].

- [180] M. Freytsis, Z. Ligeti and J. T. Ruderman, Flavor models for $\bar{B} \rightarrow D^{(*)}\tau\bar{\nu}$, *Phys. Rev. D* **92**, no. 5, 054018 (2015) [arXiv:1506.08896 [hep-ph]].
- [181] J. P. Lees *et al.* [BaBar Collaboration], Search for $B \rightarrow K^{(*)}\ell\bar{\ell}$ and invisible quarkonium decays, *Phys. Rev. D* **87**, no. 11, 112005 (2013) [arXiv:1303.7465 [hep-ex]].
- [182] O. Lutz *et al.* [Belle Collaboration], Search for $B \rightarrow h^{(*)}\nu\bar{\nu}$ with the full Belle $\Upsilon(4S)$ data sample, *Phys. Rev. D* **87**, no. 11, 111103 (2013) [arXiv:1303.3719 [hep-ex]].
- [183] A. J. Buras, J. Girrbach-Noe, C. Niehoff and D. M. Straub, $B \rightarrow K^{(*)}\nu\bar{\nu}$ decays in the Standard Model and beyond, *JHEP* **1502**, 184 (2015) [arXiv:1409.4557 [hep-ph]].
- [184] R. Aaij *et al.* [LHCb Collaboration], Search for the rare decay $D^0 \rightarrow \mu^+\mu^-$, *Phys. Lett. B* **725**, 15 (2013) [arXiv:1305.5059 [hep-ex]].
- [185] R. Aaij *et al.* [LHCb Collaboration], Measurement of the $B_s^0 \rightarrow \mu^+\mu^-$ branching fraction and search for $B^0 \rightarrow \mu^+\mu^-$ decays at the LHCb experiment, *Phys. Rev. Lett.* **111**, 101805 (2013) [arXiv:1307.5024 [hep-ex]].
- [186] F. Beaujean, C. Bobeth and S. Jahn, Constraints on tensor and scalar couplings from $B \rightarrow K\bar{\mu}\mu$ and $B_s \rightarrow \bar{\mu}\mu$, *Eur. Phys. J. C* **75**, no. 9, 456 (2015) [arXiv:1508.01526 [hep-ph]].
- [187] S. Descotes-Genon, L. Hofer, J. Matias and J. Virto, 2016, Global analysis of $b \rightarrow s\ell\ell$ anomalies, *JHEP* 06 092 arXiv:1510.04239 [hep-ph].
- [188] G. Hiller and M. Schmaltz, 2014, R_K and future $b \rightarrow s\ell\ell$ physics beyond the standard model opportunities, *Phys. Rev. D*, **90**, 054014. [arXiv:1408.1627 [hep-ph]].
- [189] W. Altmannshofer and D. M. Straub, New physics in $b \rightarrow s$ transitions after LHC run 1, *Eur. Phys. J. C* **75**, no. 8, 382 (2015) [arXiv:1411.3161 [hep-ph]].
- [190] S. Chatrchyan *et al.* [CMS Collaboration], Measurement of the $B(s)$ to $\mu^+\mu^-$ branching fraction and search for $B0$ to $\mu^+\mu^-$ with the CMS Experiment, *Phys. Rev. Lett.* **111**, 101804 (2013) [arXiv:1307.5025 [hep-ex]].

PHỤ LỤC

A. Mô hình cực tiểu với leptoquark

Mô hình có cấu trúc giống như SM cộng thêm phần mở rộng hạt là một hạt đơn tuyêն của $SU(2)_L$, mang cả số baryon và số lepton nên hạt sẽ tương tác với đồng thời với lepton và quark, có siêu tích $Y = -\frac{1}{3}$ [71]. Dưới biến đổi chuẩn $SU(3)_C \otimes SU(2)_L \otimes U(1)_Y$ leptoquark được biểu diễn như sau $(\mathbf{3}, \mathbf{1}, -\frac{1}{3})$. Lagrangian của mô hình lúc này bao gồm Lagrangian của SM cộng thêm Lagrangian của Φ ,

$$\begin{aligned} \mathcal{L}_\Phi = & (D_\mu \Phi)^\dagger D_\mu \Phi - M_\Phi^2 |\Phi|^2 - g_{h\Phi} |\phi|^2 |\Phi|^2 \\ & + \bar{Q}^c \boldsymbol{\lambda}^L i\tau_2 L \Phi^* + \bar{u}_R^c \boldsymbol{\lambda}^R e_R \Phi^* + \text{h.c.}, \end{aligned} \quad (\text{A.1})$$

trong đó ϕ là lưỡng tuyêն Higgs, $\boldsymbol{\lambda}^{L,R}$ là các ma trận trong không gian vị, và $\psi^c = C\bar{\psi}^T$ là các spinor liên hợp điện tích. Tương tác của các leptoquark được khai triển theo (A.1), cụ thể ở đây là thành phần ở dòng thứ 2. Với sự đóng góp của các tương tác mới này sẽ cho đóng góp để giải quyết vấn đề của vật lý vị. Khai triển chúng trong cơ sở các trạng thái vật lý của quark và lepton tích điện trong đó ma trận quay \mathbf{U}_f (\mathbf{V}_f) với $f_{L,R}$ là fermion phân cực trái, phải.

$$\begin{aligned} u'_L &= \mathbf{U}_u^\dagger u_L, & d'_L &= \mathbf{U}_d^\dagger d_L, & e'_L &= \mathbf{U}_e^\dagger e_L, & \nu'_L &= \mathbf{U}_\nu^\dagger \nu_L \\ u'_R &= \mathbf{V}_u^\dagger u_R, & d'_R &= \mathbf{V}_d^\dagger d_R, & e'_R &= \mathbf{V}_e^\dagger e_R, & \nu'_R &= \mathbf{V}_\nu^\dagger \nu_R \end{aligned} \quad (\text{A.2})$$

Ta có

$$\mathcal{L}_\Phi \ni \bar{u}_L^c \boldsymbol{\lambda}_{ue}^L e_L \Phi^* - \bar{d}_L^c \boldsymbol{\lambda}_{d\nu}^L \nu_L \Phi^* + \bar{u}_R^c \boldsymbol{\lambda}_{ue}^R e_R \Phi^* + \text{h.c.}, \quad (\text{A.3})$$

trong đó

$$\boldsymbol{\lambda}_{ue}^L = \mathbf{U}_u^T \boldsymbol{\lambda}^L \mathbf{U}_e, \quad \boldsymbol{\lambda}_{d\nu}^L = \mathbf{U}_d^T \boldsymbol{\lambda}^L, \quad \boldsymbol{\lambda}_{ue}^R = \mathbf{V}_u^T \boldsymbol{\lambda}_R \mathbf{V}_e, \quad (\text{A.4})$$

và ma trận CKM và ma trận PMNS

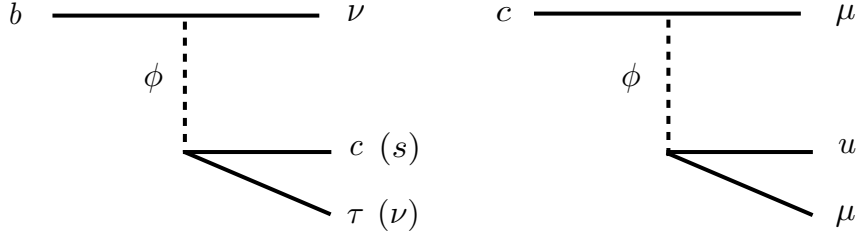
$$\mathbf{V}_{\text{CKM}} = \mathbf{U}_u^\dagger \mathbf{U}_d, \quad \mathbf{U}_{\text{PMNS}} = \mathbf{U}_\nu^\dagger \mathbf{U}_e. \quad (\text{A.5})$$

Vì số lepton là bảo toàn trong phần lepton mang điện ở gần đúng cây nên \mathbf{U}_e có thể coi ma trận là bằng ma trận đơn vị, dẫn tới $\mathbf{U}_{\text{PMNS}} = \mathbf{U}_\nu$.

Với số hạng thứ 1 và 3 trong (A.3) sẽ cho chúng ta đóng góp vào quá trình rã bán lepton B meson với leptoquark làm trung gian ở ngay ở gần đúng cây, được mô tả trong hình 16. Lagrangian hiệu dụng cho quá trình này có dạng

$$\begin{aligned} \mathcal{L}_{\text{eff}}^{(\Phi)} = & \frac{1}{2M_\Phi^2} \left[-\lambda_{u_i \ell_j}^{L*} \lambda_{b\nu_k}^L \bar{u}_L^i \gamma_\mu b_L \bar{\ell}_L^j \gamma^\mu \nu_L^k \right. \\ & \left. + \lambda_{u_i \ell_j}^{R*} \lambda_{b\nu_k}^L \left(\bar{u}_R^i b_L \bar{\ell}_R^j \nu_L^k - \frac{\bar{u}_R^i \sigma_{\mu\nu} b_L \bar{\ell}_R^j \sigma^{\mu\nu} \nu_L^k}{4} \right) \right], \end{aligned} \quad (\text{A.6})$$

trong đó i, j, k là các chỉ số vị. Khai triển chúng trong hệ cơ sở các trạng thái vật lý thì thành phần đầu tiên sẽ tạo ra các đóng góp tỷ lệ với các phần tử của ma trận CKM \mathbf{V}_{ub} và \mathbf{V}_{cb} .



Hình 16: Giản đồ mức cây đóng góp vào phân rã yếu.

Các hệ số $V_{ub}V_{cb}$ với vị lepton khác nhau là khác nhau vì nó tỷ lệ với $\lambda_{u_i \ell_j}^{L*} \lambda_{b\nu_k}^L$, hay đổi với vị $l_j \nu_k$ thì các hằng số tương tác này là khác nhau. Thành phần thứ hai bao gồm các tương tác mới không có trong mô hình chuẩn. Chính vì vậy nó có thể giúp giải thích được tất cả các tỷ số rã từ phân rã B-meson.

Một trong kênh rã đang được chú ý hiện nay là kênh rã $\bar{B} \rightarrow D^{(*)}\tau\bar{\nu}$. Thực nghiệm cho thấy rằng tỷ số rã này là lớn hơn khoảng 30% so với tiên đoán của SM. Bằng một phân tích độc lập không phụ thuộc vào mô hình thì người ta đã tính toán toán tử hiệu dụng và cho sự ảnh hưởng của các toán tử hiệu dụng này khi mà cho chạy từ $\mu = M_\Phi$ đến $\mu = m_b$ [179, 180]. Ở bài báo sau cùng, người ta tìm ra được một kết quả cho các hằng số tương tác mới là phù hợp rất tốt với thực nghiệm cho tỷ số rã $\bar{B} \rightarrow D^{(*)}\tau\bar{\nu}$

$$\lambda_{c\tau}^{L*} \lambda_{b\nu_\tau}^L \approx 0.35 \hat{M}_\Phi^2, \quad \lambda_{c\tau}^{R*} \lambda_{b\nu_\tau}^L \approx -0.03 \hat{M}_\Phi^2, \quad (\text{A.7})$$

với giả sử rằng chỉ có neutrino ν_τ là liên quan đến quá trình rã (vì có biên độ lớn và do đó tạo ra hiệu ứng lớn). Trong mô hình với vô hướng đơn tuyến leptoquark, $\hat{M}_\Phi \equiv M_\Phi/\text{TeV}$. Như vậy, với khối lượng leptoquark ở gần thang TeV thì $\lambda_{c\tau}^{L*} \lambda_{b\nu_\tau}^L$ cỡ bậc $\mathcal{O}(1)$ và các hằng số tương tác của leptoquark phân cực phải là nhỏ hơn rất nhiều so với các hằng số tương tác của các leptoquark phân cực trái.

Ngoài ra trong mô hình này cũng xuất hiện dòng trung hòa thay đổi vị ở gần đúng cây và thể hiện thông qua Hình 16. Hình 16 cho phép giải thích các tỷ số rã $\bar{B} \rightarrow \bar{K}\nu\bar{\nu}$ và $D^0 \rightarrow \mu^+\mu^-$. Cụ thể toán tử Lagragian hiệu dụng mô tả cho kênh rã $\bar{B} \rightarrow \bar{K}\nu\bar{\nu}$ có dạng

$$\mathcal{L}_{\text{eff}}^{(\Phi)} = \frac{1}{2M_\Phi^2} \lambda_{s\nu_i}^{L*} \lambda_{b\nu_j}^L \bar{s}_L \gamma_\mu b_L \bar{\nu}_L^i \gamma^\mu \nu_L^j. \quad (\text{A.8})$$

Công thức (A.8) cho phép ta xác định tỷ số rã $R_{\nu\bar{\nu}} = \Gamma/\Gamma_{\text{SM}}$ với đóng góp của hạt leptoquark dưới dạng

$$R_{\nu\bar{\nu}}^{(\Phi)} = 1 - \frac{2r}{3} \text{Re} \frac{(\lambda^L \lambda^{L\dagger})_{bs}}{V_{tb} V_{ts}^*} + \frac{r^2}{3} \frac{(\lambda^L \lambda^{L\dagger})_{bb} (\lambda^L \lambda^{L\dagger})_{ss}}{|V_{tb} V_{ts}^*|^2}, \quad (\text{A.9})$$

trong đó $(\lambda^L \lambda^{L\dagger})_{bs} = \sum_i \lambda_{b\nu_i}^L \lambda_{s\nu_i}^{L*} \dots$, và

$$r = \frac{s_W^4}{2\alpha^2} \frac{1}{X_0(x_t)} \frac{m_W^2}{M_\phi^2} \approx \frac{1.91}{\hat{M}_\phi^2}. \quad (\text{A.10})$$

Tại đây $X_0(x_t) = \frac{x_t(2+x_t)}{8(x_t-1)} + \frac{3x_t(x_t-2)}{8(1-x_t)^2} \ln x_t \approx 1.48$ với $x_t = m_t^2/m_W^2$, $s_W^2 = 0.2313$ là bình phương của góc trộn yếu. Một trong những ràng buộc rất mạnh mẽ là tỷ số rã $B^- \rightarrow K^-\nu\bar{\nu}$

và $B^- \rightarrow K^{*-} \nu \bar{\nu}$ được đưa ra bởi BaBar [181] và Belle [182], đưa đến ràng buộc $R_{\nu \bar{\nu}} < 4.3$ và $R_{\nu \bar{\nu}} < 4.4$ tại 90% CL [183]. sử dụng bất đẳng thức Schwarz, người ta thu được từ công thức (A.9)

$$-1.20 \hat{M}_\Phi^2 < \text{Re} \frac{(\lambda^L \lambda^{L\dagger})_{bs}}{V_{tb} V_{ts}^*} < 2.25 \hat{M}_\Phi^2. \quad (\text{A.11})$$

Quá trình FCNC trong kênh rã $D^0 \rightarrow \mu^+ \mu^-$ có thể xuất hiện ở gần đúng cây trong mô hình của chúng ta. Ở đây chúng ta giả thiết rằng trong SM không có sự đóng góp của kênh rã $D^0 \rightarrow \mu^+ \mu^-$. Người ta tìm thấy tỷ số rã từ các tương tác hiệu dụng đưa ra bởi phương trình A.8, chúng tôi tìm thấy tốc độ phân rã

$$\begin{aligned} \Gamma = & \frac{f_D^2 m_D^3}{256 \pi M_\Phi^4} \left(\frac{m_D}{m_c} \right)^2 \beta_\mu \left[\beta_\mu^2 \left| \lambda_{c\mu}^L \lambda_{u\mu}^{R*} - \lambda_{c\mu}^R \lambda_{u\mu}^{L*} \right|^2 \right. \\ & \left. + \left| \lambda_{c\mu}^L \lambda_{u\mu}^{R*} + \lambda_{c\mu}^R \lambda_{u\mu}^{L*} + \frac{2m_\mu m_c}{m_D^2} (\lambda_{c\mu}^L \lambda_{u\mu}^{L*} + \lambda_{c\mu}^R \lambda_{u\mu}^{R*}) \right|^2 \right], \end{aligned} \quad (\text{A.12})$$

trong đó $f_D = 212(1)$ MeV là hằng số phân rã meson D và $\beta_\mu = (1 - 4m_\mu^2/m_D^2)^{1/2}$. Chúng tôi sử dụng khối lượng quark charm đang chạy cõi $m_c \equiv m_c(M_\Phi) \approx 0,54$ GeV, $M_\Phi \sim 1$ TeV. Với những giả thiết như vậy và sử dụng giới hạn trên thực nghiệm $\text{Br}(D^0 \rightarrow \mu^+ \mu^-) < 7.6 \cdot 10^{-9}$ (tại 95% CL) [184] ta thu được điều kiện ràng buộc

$$\begin{aligned} \sqrt{\left| \lambda_{c\mu}^L \right|^2 \left| \lambda_{u\mu}^R \right|^2 + \left| \lambda_{c\mu}^R \right|^2 \left| \lambda_{u\mu}^L \right|^2} &< 1.2 \cdot 10^{-3} \hat{M}_\Phi^2, \\ \left| \lambda_{c\mu}^L \lambda_{u\mu}^{L*} + \lambda_{c\mu}^R \lambda_{u\mu}^{R*} \right| &< 0.051 \hat{M}_\Phi^2. \end{aligned} \quad (\text{A.13})$$

Như vậy với phương trình A.7 cho chúng ta ràng buộc về giải quyết tỷ số rã $\bar{B} \rightarrow D^{(*)} \tau \bar{\nu}$, phương trình A.11 cho ràng buộc về tỷ số rã và phương trình A.13 cho ràng buộc về tỷ số rã $D^0 \rightarrow \mu^+ \mu^-$. Như vậy chúng ta có 3 điều kiện ràng buộc về các hằng số tương tác của leptoquark phân cực trái và phải λ^L, λ^R . Ở đây chúng ta thấy nếu như λ^L cõi vào bậc $\mathcal{O}(1)$, λ^R nhỏ hơn rất nhiều so với λ^L thì tự động giải quyết về thực nghiệm các tỷ số rã $\bar{B} \rightarrow D^{(*)} \tau \bar{\nu}$, $B^- \rightarrow K^{*-} \nu \bar{\nu}$ và $D^0 \rightarrow \mu^+ \mu^-$.

Mô hình tiếp tục đi khảo sát kênh rã $b \rightarrow s \ell^+ \ell^-$ nhằm giải thích các kết quả thực nghiệm tại LHCb

$$R_K^{\text{LHCb}} ([1.1, 6] \text{ GeV}^2) = 0.745^{+0.090}_{-0.074} \pm 0.036,$$

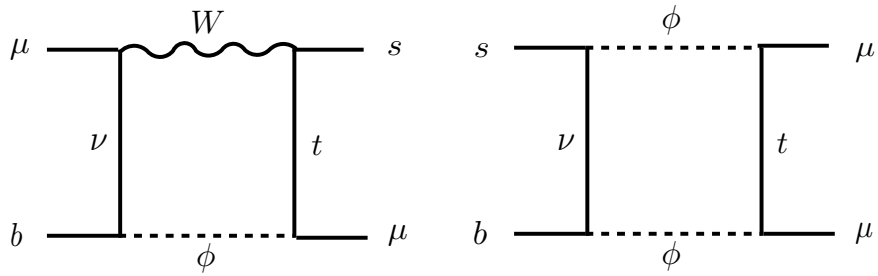
với khối lượng bất biến của cặp lepton đi ra là ($1.0 \leq q^2 \leq 6.0$ GeV 2). Kết quả này được nhóm tác giả R. Aaij công bố trên tạp chí Phys. Rev. Lett. năm 2014.

Trong một phân tích không phụ thuộc vào mô hình [188] để giải thích dữ liệu người ta sử dụng hàm Hamiltonian hiệu dụng

$$\mathcal{H}_{\text{eff}} = -\frac{4G_F}{\sqrt{2}} V_{tb} V_{ts}^* \frac{\alpha_e}{4\pi} \sum_i C_i(\mu) \mathcal{O}_i(\mu), \quad (\text{A.14})$$

với các toán tử dạng V, A mô tả quá trình $b \rightarrow s \ell \ell$ ứng với các lepton mang điện

$$\mathcal{O}_9 = [\bar{s} \gamma_\mu P_L b] [\bar{\ell} \gamma^\mu \ell], \quad \mathcal{O}_{10} = [\bar{s} \gamma_\mu P_L b] [\bar{\ell} \gamma^\mu \gamma_5 \ell], \quad (\text{A.15})$$



Hình 17: Giản đồ hộp đóng góp vào dịch chuyển $b \rightarrow s\mu^+\mu^-$.

với

$$\mathcal{O}_{LL}^\ell \equiv (\mathcal{O}_9^\ell - \mathcal{O}_{10}^\ell)/2, \quad \mathcal{O}_{LR}^\ell \equiv (\mathcal{O}_9^\ell + \mathcal{O}_{10}^\ell)/2, \quad (\text{A.16})$$

do đó

$$C_{LL}^\ell = C_9^\ell - C_{10}^\ell, \quad C_{LR}^\ell = C_9^\ell + C_{10}^\ell. \quad (\text{A.17})$$

Trong mô hình cực tiêu với leptoquark, dị thường R_K có thể nhận được từ bối đính một vòng của các hạt leptoquark được mô tả bởi hai giản đồ trong Hình 17. Một giản đồ với các đường trong là hạt gauge boson W và hạt leptoquark Φ . Một giản đồ với các đường trong chỉ là hạt leptoquark Φ . Hai giản đồ sẽ cho đóng góp vào các hệ số Wilson. Trong giới hạn $M_\Phi^2 \gg m_{t,W}^2$, chúng ta thu được cho các đóng góp vào hệ số Wilson [188]

$$\begin{aligned} C_{LL}^{\mu(\Phi)} &= \frac{m_t^2}{8\pi\alpha M_\Phi^2} |\lambda_{t\mu}^L|^2 \\ &\quad - \frac{1}{64\pi\alpha} \frac{\sqrt{2}}{G_F M_\Phi^2} \frac{(\lambda^L \lambda^{L\dagger})_{bs}}{V_{tb} V_{ts}^*} (\lambda^{L\dagger} \lambda^L)_{\mu\mu}, \\ C_{LR}^{\mu(\Phi)} &= \frac{m_t^2}{16\pi\alpha M_\Phi^2} |\lambda_{t\mu}^R|^2 \left[\ln \frac{M_\Phi^2}{m_t^2} - f(x_t) \right] \\ &\quad - \frac{1}{64\pi\alpha} \frac{\sqrt{2}}{G_F M_\Phi^2} \frac{(\lambda^L \lambda^{L\dagger})_{bs}}{V_{tb} V_{ts}^*} (\lambda^{R\dagger} \lambda^R)_{\mu\mu}, \end{aligned} \quad (\text{A.18})$$

trong đó $m_t \equiv m_t(m_t) \approx 162,3$ GeV là khối lượng của top quark và $f(x_t) = 1 + \frac{3}{x_t - 1} (\frac{\ln x_t}{x_t - 1} - 1) \approx 0,47$. Khi nghiên cứu độc lập với mô hình, điều kiện để có thể giải thích tốt nhất các kết thực nghiệm về các tỷ số R_K, R_{K^*} thì tương ứng với $-1,5 < C_{LL}^\mu < -0,7$ và $C_{LR}^\mu \approx 0$ tại thang năng lượng $\mu \sim M_\Phi$ [188]. Và ở đây với dữ liệu của chúng tôi thì trong mô hình này sẽ có $C_{LL}^\mu \approx -1$ và $C_{LR}^\mu \approx 0$. Điều này hoàn toàn đồng thuận với tài liệu [178, 186, 187, 189]. Với giả thiết trên thì mô hình không chỉ giải quyết tốt vấn đề R_K, R_{K^*} mà thậm chí nó còn có thể giải thích tốt vấn đề tỷ số $\text{Br}(B_s \rightarrow \mu^+\mu^-)/\text{Br}(B_s \rightarrow \mu^+\mu^-)_{\text{SM}} = 0.79 \pm 0.20$ được đưa ra bởi LHCb [185] và CMS [190].

Các đóng góp từ giản đồ hộp $W-\Phi$ hõn hợp trong (A.18) bị ràng buộc bởi các liên kết của leptoquark với top-quark và muon. Các đại lượng này được dự đoán là dương trong mô hình và do đó riêng chúng không thể giải thích được dị thường R_K . Các đóng góp từ giản đồ hộp với hai leptoquark Φ là đường trong là cần thiết để tái tạo giá trị chuẩn $C_{LL}^\mu \approx -1$.

Điều này đòi hỏi

$$\sum_i |\lambda_{u_i \mu}^L|^2 \operatorname{Re} \frac{(\lambda^L \lambda^{L\dagger})_{bs}}{V_{tb} V_{ts}^*} - 1.74 |\lambda_{t\mu}^L|^2 \approx 12.5 \hat{M}_\phi^2. \quad (\text{A.19})$$

Để thu được $C_{LR}^\mu \approx 0$ thì đóng góp của các hằng số tương tác với các leptoquark phân cực phải nhỏ hơn nhiều so với các leptoquark phân cực trái. Kết hợp (A.19) với giới hạn trên trong A.11 tạo ra

$$\sqrt{|\lambda_{u\mu}^L|^2 + |\lambda_{c\mu}^L|^2 + \left(1 - \frac{0.77}{\hat{M}_\phi^2}\right) |\lambda_{t\mu}^L|^2} > 2.36, \quad (\text{A.20})$$

Như vậy ở đây ta cũng thu được với khối lượng của leptoquark ở thang TeV thì các hệ số tương tác $\lambda_{t\mu}^L, \lambda_{u\mu}^L, \lambda_{c\mu}^L$ rơi vào bậc $\mathcal{O}(1)$ của M_Φ , các hằng số tương tác với các leptoquark phân cực phải là nhỏ. Điều này hoàn toàn phù hợp với không gian tham số trong trường hợp R_D, R_{D^*} . Với $C_{LL}^\mu = -0.7$ hoặc -1.5 thay thế cho -1 thì về phải của giới hạn này phải bằng 2.0 hoặc 2.9.

Như vậy bằng các kết quả lập luận [71], mô hình cực tiểu với một vô hướng đơn tuyến leptoquark sẽ cho chúng ta giải thích được đồng thời tỷ số R_D, R_{D^*} và R_K, R_{K^*} .

Mô hình cũng giải thích được cho dao động $B_s - \bar{B}_s$. Tỷ lệ $(\lambda^L \lambda^{L\dagger})_{bs}/(V_{tb} V_{ts}^*)$ trong (A.19) cũng có thể bị giới hạn bởi các phép đo hiện có của biên độ trộn $B_s - \bar{B}_s$. Đóng góp của leptoquark vào hệ số lưỡng cực $C_{7\gamma}$ cho sự phân rã $\bar{B} \rightarrow X_s \gamma$ dẫn đến

$$C_{7\gamma} = C_{7\gamma}^{\text{SM}} + \left(\frac{v}{12M_\Phi}\right)^2 \frac{(\lambda^L \lambda^{L\dagger})_{bs}}{V_{tb} V_{ts}^*}. \quad (\text{A.21})$$

Mỗi quan hệ [71] ngũ ý rằng sự thay đổi tương ứng trong tỷ lệ phân nhánh $\bar{B} \rightarrow X_s \gamma$ nhỏ hơn khoảng 1% và do đó an toàn dưới giới hạn thực nghiệm. Mô hình thậm chí cũng giải thích được mômen từ dị thường của muon [71].

B. Các tham số xuất hiện trong ma trận khối lượng lepton

Khai triển của các hàm $f_{ab}^{EE}, f_{ab}^{eE}, f_{ab}^{ee}, f_{1b}^{e\xi}, f_{1b}^{E\xi}$ trong ma trận trộn khối lượng lepton \mathcal{M}_l được đưa ra bởi

$$f_{\alpha b}^{ee} = -\frac{1}{\sqrt{2}} s_{\alpha b}^e v', \quad (\text{B.1})$$

$$f_{1b}^{ee} = -\frac{1}{\sqrt{2}} \frac{s_{1b}^e}{\Lambda} v' w - \frac{1}{\sqrt{2}} \frac{s_{1b}'^e}{\Lambda} v w' - \frac{h_{1b}^e}{2\sqrt{2}\Lambda v' w'}, \quad (\text{B.2})$$

$$f_{\alpha b}^{EE} = -\frac{1}{\sqrt{2}} s_{\alpha b}^E w', \quad (\text{B.3})$$

$$f_{1b}^{EE} = -\frac{1}{2} \frac{s_{1b}^E}{\Lambda} w w' - \frac{1}{2} \frac{s_{1b}'^E}{\Lambda} w'^2, \quad (\text{B.4})$$

$$f_{\alpha b}^{eE} = -\frac{1}{\sqrt{2}} h_{\alpha b}^E v' - \frac{1}{\sqrt{2}} s_{\alpha b}^E v, \quad (\text{B.5})$$

$$f_{\alpha b}^{Ee} = -\frac{1}{\sqrt{2}} s_{\alpha b}^e w - \frac{1}{\sqrt{2}} h_{\alpha b}^e w', \quad (\text{B.6})$$

$$f_{1b}^{eE} = -\frac{1}{\sqrt{2}} \frac{h_{1b}^E}{\Lambda} v' w - \frac{1}{2\sqrt{2}} \frac{s_{1b}^E}{\Lambda} (v' w' + v w) - \frac{1}{\sqrt{2}} \frac{s_{1b}'^E}{\Lambda} v w', \quad (\text{B.7})$$

$$f_{1b}^{Ee} = -\frac{1}{2\Lambda} h_{1b}^e w w' - \frac{1}{2\Lambda} s_{1b}^e w^2 - \frac{1}{2\Lambda} s_{1b}'^e w'^2, \quad (\text{B.8})$$

$$f_{1b}^{\xi e} = -\frac{1}{2\Lambda} s'_{1b} v^2 - \frac{1}{2\Lambda} s_{1b}^e v'^2 - \frac{1}{2\Lambda} h_{1b}^e v v' + \delta_{1b} f_{11}^{e\xi}, \quad (\text{B.9})$$

$$f_{b1}^{e\xi} = \delta_{1b} f_{11}^{e\xi}, \quad (\text{B.10})$$

$$f_{1b}^{\xi E} = -\frac{1}{2\Lambda} s'_{1b} v^2 - \frac{1}{2\Lambda} s_{1b}^E v v' + \frac{1}{2\Lambda} h_{1b}^E v'^2 + \delta_{1b} f_{11}^{E\xi}, \quad (\text{B.11})$$

$$f_{b1}^{E\xi} = \delta_{b1} f_{11}^{E\xi}, \quad (\text{B.12})$$

$$f^{\xi\xi} = s_{11} w w' + s'_{11} w'^2. \quad (\text{B.13})$$

với

$$f_{11}^{e\xi} = -\left(h_{11}^\xi\right)^* \frac{\sqrt{2}}{\Lambda} w v' - \left(s'_{11}\right)^* \frac{\sqrt{2}}{\Lambda} v w' - \frac{\left(s_{11}\right)^*}{\sqrt{2}\Lambda} (v w + v' w'), \quad (\text{B.14})$$

$$f_{11}^{E_1\xi} = \frac{\left(h_{11}^\xi\right)^*}{\sqrt{2}\Lambda} (v')^2 + \frac{\left(s'_{11}\right)^*}{\sqrt{2}\Lambda} v^2 + \frac{\left(s_{11}\right)^*}{\sqrt{2}\Lambda} v v'. \quad (\text{B.15})$$

C. Hàm $\Gamma^{f_i f_j f_k}$

$$\Gamma^{WZ^{e_b}} = (m_Z^2 - m_W^2) \left(1 + \frac{1}{\epsilon} - \gamma + \ln 4\pi - \ln m_{e_b}^2\right) - m_Z^2 \frac{\ln x_Z^{e_b}}{x_Z^{e_b} - 1} + m_W^2 \frac{\ln x_W^{e_b}}{x_W^{e_b} - 1}, \quad (\text{C.1})$$

$$\Gamma^{WZ^{\nu_a}} = (m_Z^2 - m_W^2) \left(1 + \frac{1}{\epsilon} - \gamma + \ln 4\pi - \ln m_{\nu_a}^2\right) - m_Z^2 \frac{\ln x_Z^{\nu_a}}{x_Z^{\nu_a} - 1} + m_W^2 \frac{\ln x_W^{\nu_a}}{x_W^{\nu_a} - 1}, \quad (\text{C.2})$$

$$\Gamma_Z^{W\nu_a e_b} = (m_{e_b}^2 - m_{\nu_a}^2) \left(1 + \frac{1}{\epsilon} - \gamma + \ln 4\pi - \ln m_Z^2\right) - m_{e_b}^2 \frac{\ln x_{e_b}^Z}{x_{e_b}^Z - 1} + m_{\nu_a}^2 \frac{\ln x_{\nu_a}^Z}{x_{\nu_a}^Z - 1}, \quad (\text{C.3})$$

$$\Gamma_{Z'}^{W\nu_a e_b} = (m_{e_b}^2 - m_{\nu_a}^2) \left(1 + \frac{1}{\epsilon} - \gamma + \ln 4\pi - \ln m_{Z'}^2\right) - m_{e_b}^2 \frac{\ln x_{e_b}^{Z'}}{x_{e_b}^{Z'} - 1} + m_{\nu_a}^2 \frac{\ln x_{\nu_a}^{Z'}}{x_{\nu_a}^{Z'} - 1}, \quad (\text{C.4})$$

$$\Gamma^{W\gamma e_c} = \left(1 + \frac{1}{\epsilon} - \gamma + \ln 4\pi - \ln m_{e_c}^2\right) - \frac{\ln x_W^{e_c}}{x_W^{e_c} - 1}, \quad (\text{C.5})$$

$$\Gamma^{XY E_c} = (m_X^2 - m_Y^2) \left(1 + \frac{1}{\epsilon} - \gamma + \ln 4\pi - \ln m_{E_c}^2\right) - m_X^2 \frac{\ln x_X^{E_c}}{x_X^{E_c} - 1} + m_Y^2 \frac{\ln x_Y^{E_c}}{x_Y^{E_c} - 1}, \quad (\text{C.6})$$

$$\Gamma^{XY \xi^0} = (m_X^2 - m_Y^2) \left(1 + \frac{1}{\epsilon} - \gamma + \ln 4\pi - \ln m_{\xi^0}^2\right) - m_X^2 \frac{\ln x_X^{\xi^0}}{x_X^{\xi^0} - 1} + m_Y^2 \frac{\ln x_Y^{\xi^0}}{x_Y^{\xi^0} - 1}, \quad (\text{C.7})$$

$$\Gamma^{XY \xi} = (m_X^2 - m_Y^2) \left(1 + \frac{1}{\epsilon} - \gamma + \ln 4\pi - \ln m_\xi^2\right) - m_X^2 \frac{\ln x_X^\xi}{x_X^\xi - 1} + m_Y^2 \frac{\ln x_Y^\xi}{x_Y^\xi - 1}, \quad (\text{C.8})$$

$$\Gamma^{XY U_c} = (m_X^2 - m_Y^2) \left(1 + \frac{1}{\epsilon} - \gamma + \ln 4\pi - \ln m_{U_c}^2\right) - m_X^2 \frac{\ln x_X^{U_c}}{x_X^{U_c} - 1} + m_Y^2 \frac{\ln x_Y^{U_c}}{x_Y^{U_c} - 1}, \quad (\text{C.9})$$

với $x_b^a = \frac{m_a^2}{m_b^2}$.

D. Hàm $\Gamma^{f_i f_j}$

$$\begin{aligned}
\Gamma^{U_l E_c} &= \left[\frac{(x_X^{U_l})^2}{(x_X^{U_l} - x_X^{E_c})(x_X^{U_l} - 1)} - \frac{(x_Y^{U_l})^2}{(x_Y^{U_l} - x_Y^{E_c})(x_Y^{U_l} - 1)} \right] \ln m_{U_l} \\
&- \left[\frac{(x_X^{E_c})^2}{(x_X^{E_c} - x_X^{U_l})(x_X^{E_c} - 1)} - \frac{(x_Y^{E_c})^2}{(x_Y^{E_c} - x_Y^{U_l})(x_Y^{E_c} - 1)} \right] \ln m_{E_c} \\
&+ \frac{x_X^{U_l} x_X^{E_c}}{(x_X^{U_l} - 1)(x_X^{E_c} - 1)} \ln m_X - \frac{x_Y^{U_l} x_Y^{E_c}}{(x_Y^{U_l} - 1)(x_Y^{E_c} - 1)} \ln m_Y
\end{aligned} \tag{D.1}$$

$$\begin{aligned}
\Gamma^{U_l \xi^0} &= \left[\frac{(x_X^{U_l})^2}{(x_X^{U_l} - x_X^{\xi^0})(x_X^{U_l} - 1)} - \frac{(x_Y^{U_l})^2}{(x_Y^{U_l} - x_Y^{\xi^0})(x_Y^{U_l} - 1)} \right] \ln m_{U_l} \\
&- \left[\frac{(x_X^{\xi^0})^2}{(x_X^{\xi^0} - x_X^{U_l})(x_X^{\xi^0} - 1)} - \frac{(x_Y^{\xi^0})^2}{(x_Y^{\xi^0} - x_Y^{U_l})(x_Y^{\xi^0} - 1)} \right] \ln m_{\xi^0} \\
&+ \frac{x_X^{U_l} x_X^{\xi^0}}{(x_X^{U_l} - 1)(x_X^{\xi^0} - 1)} \ln m_X - \frac{x_Y^{U_l} x_Y^{\xi^0}}{(x_Y^{U_l} - 1)(x_Y^{\xi^0} - 1)} \ln m_Y
\end{aligned} \tag{D.2}$$

$$\begin{aligned}
\Gamma^{U_l \xi} &= \left[\frac{(x_X^{U_l})^2}{(x_X^{U_l} - x_X^{\xi})(x_X^{U_l} - 1)} - \frac{(x_Y^{U_l})^2}{(x_Y^{U_l} - x_Y^{\xi})(x_Y^{U_l} - 1)} \right] \ln m_{U_l} \\
&- \left[\frac{(x_X^{\xi})^2}{(x_X^{\xi} - x_X^{U_l})(x_X^{\xi} - 1)} - \frac{(x_Y^{\xi})^2}{(x_Y^{\xi} - x_Y^{U_l})(x_Y^{\xi} - 1)} \right] \ln m_{\xi} \\
&+ \frac{x_X^{U_l} x_X^{\xi}}{(x_X^{U_l} - 1)(x_X^{\xi} - 1)} \ln m_X - \frac{x_Y^{U_l} x_Y^{\xi}}{(x_Y^{U_l} - 1)(x_Y^{\xi} - 1)} \ln m_Y
\end{aligned} \tag{D.3}$$

với $x_b^a = \frac{m_a^2}{m_b^2}$.